Supporting Information

Preparation of Metal Oxides Containing ppm Levels of Pd as Catalysts for the Reduction of Nitroarene and Evaluation of Their Catalytic Activity by the Fluorescence-Based High-Throughput Screening Method

Taeho Lim and Min Su Han *

Department of Chemistry, Gwangju Institute of Science and Technology (GIST), Gwangju 61005, Korea; thlim0323@gist.ac.kr

* Correspondence: happyhan@gist.ac.kr; Tel: +062-715-2850

Received: 20 April 2020; Accepted: 09 May 2020; Published: date

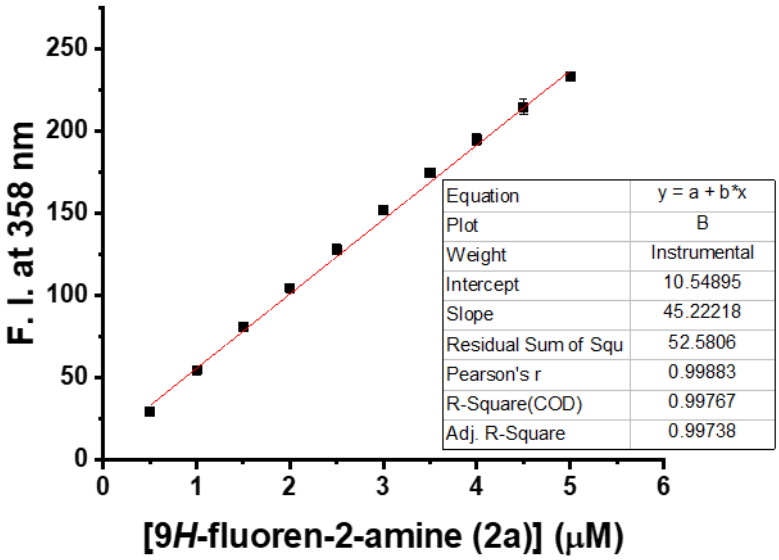

Fig. S1. Plot of fluorescence intensity at 358 nm versus various concentration of **2a** in toluene (λ_{ex} = 294 nm, three replicates) and the standard curve (red line). The equation of the standrad curve is in the table (Concentration of **2a**=(F_{358}–10.54895)/45.22218).

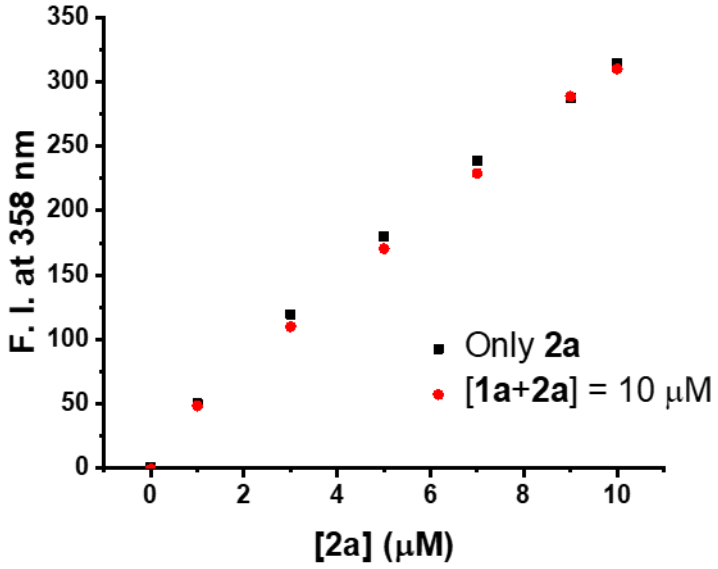

Fig. S2. Plot of fluorescence intensity at 358 nm versus various concentration of **2a** in toluene (λ_{ex} = 294 nm, black: only **2a**, red: [**1a**+**2a**] = 10 μM). The fluorescence of **2a** is the same whether or not **1a** is present. Using different fluorescence spectrophotometer, the intensity is different from Fig. S1.

Table S1. Summary of XRD results of metal oxides

Metal	Metal oxide (by XRD)	Reference
Mg	MgO	[1]
Cr	Cr_2O_3	[2]
Mn	Mn_2O_3	[3]
Fe	Fe_2O_3	[2]
Co	Co_3O_4	[2]
Ni	NiO	[2]
Zn	ZnO	[4]

Al	Al_2O_3	[5]
Sr	$SrCO_3$	[6
Ce	CeO_2	[2]
Zr	ZrO	[7]
Cd	CdO	[8]
In	In_2O_3	[9]
Sn	SnO_2	[10]
Ca	$CaO + CaCO_3$	[11]
Y	Y_2O_3	[12]
Cu	CuO	[13]

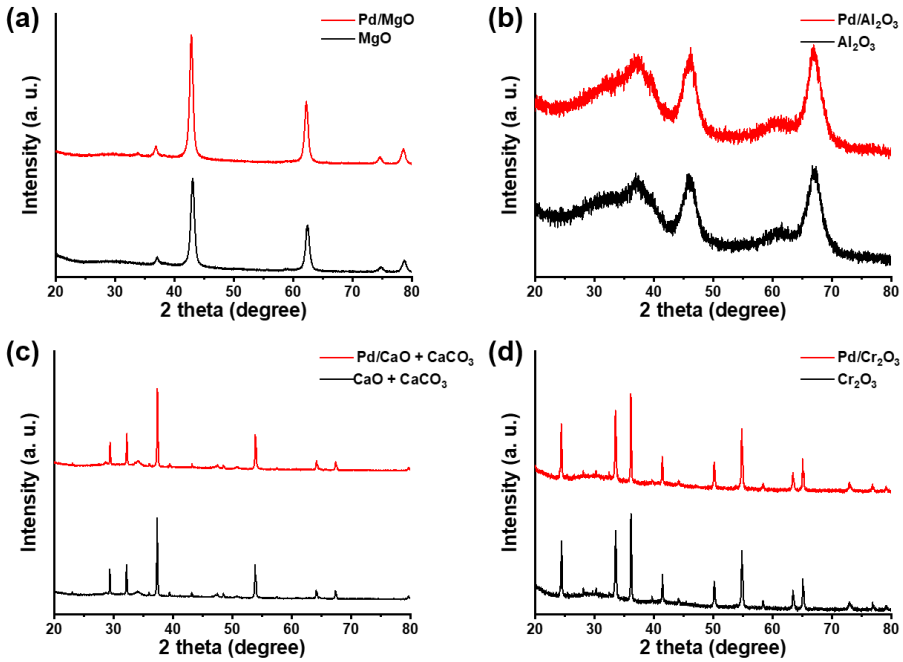

Fig. S3. XRD pattern of metal oxides. (a) MgO (black line) and Pd/MgO (red line). (b) Al_2O_3 (black line) and Pd/Al_2O_3 (red line). (c) CaO + $CaCO_3$ (black line) and Pd/CaO + $CaCO_3$ (red line). (d) Cr_2O_3 (black line) and Pd/Cr_2O_3 (red line).

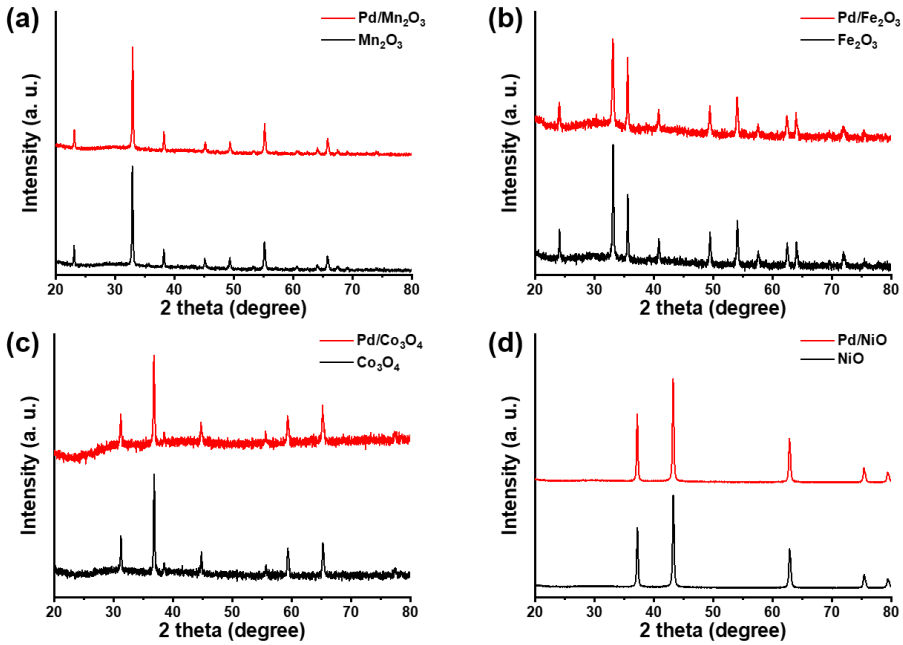

Fig. S4. XRD pattern of metal oxides. (a) Mn_2O_3 (black line) and Pd/Mn_2O_3 (red line). (b) Fe_2O_3 (black line) and Pd/Fe_2O_3 (red line). (c) Co_3O_4 (black line) and Pd/Co_3O_4 (red line). (d) NiO (black line) and Pd/NiO (red line).

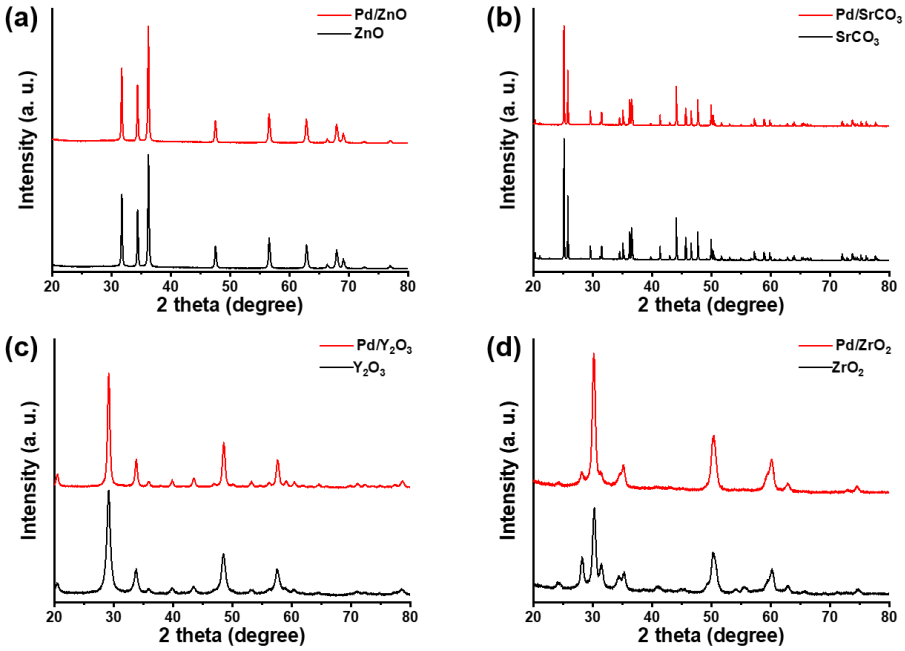

Fig. S5. XRD pattern of metal oxides. (a) ZnO (black line) and Pd/ZnO (red line). (b) $SrCO_3$ (black line) and Pd/$SrCO_3$ (red line). (c) Y_2O_3 (black line) and Pd/Y_2O_3 (red line). (d) ZrO_2 (black line) and Pd/ZrO_2 (red line).

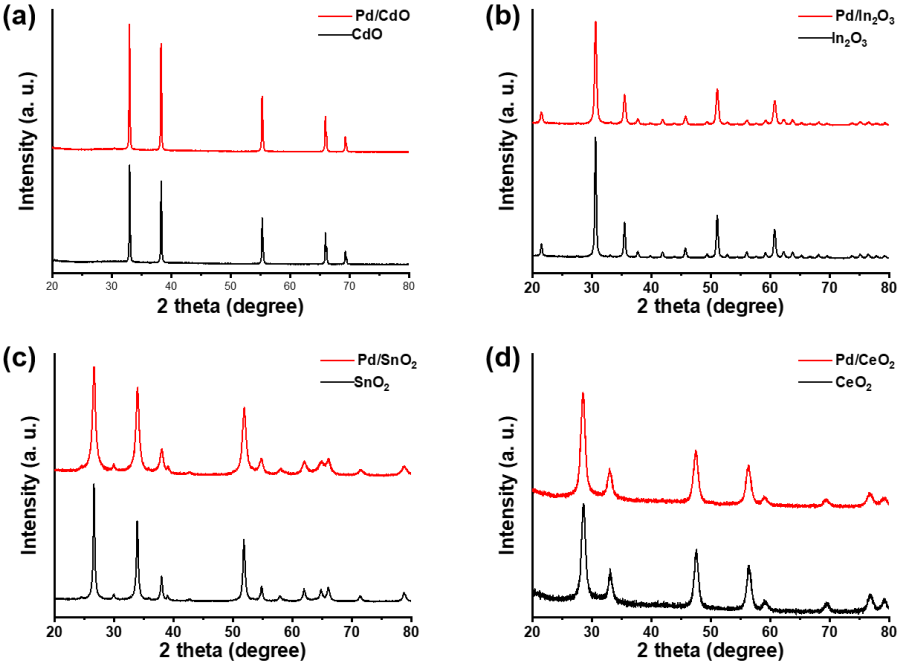

Fig. S6. XRD pattern of metal oxides. (a) CdO (black line) and Pd/CdO (red line). (b) In_2O_3 (black line) and Pd/In_2O_3 (red line). (c) SnO_2 (black line) and Pd/SnO_2 (red line).

(d) CeO_2 (black line) and Pd/CeO_2 (red line).

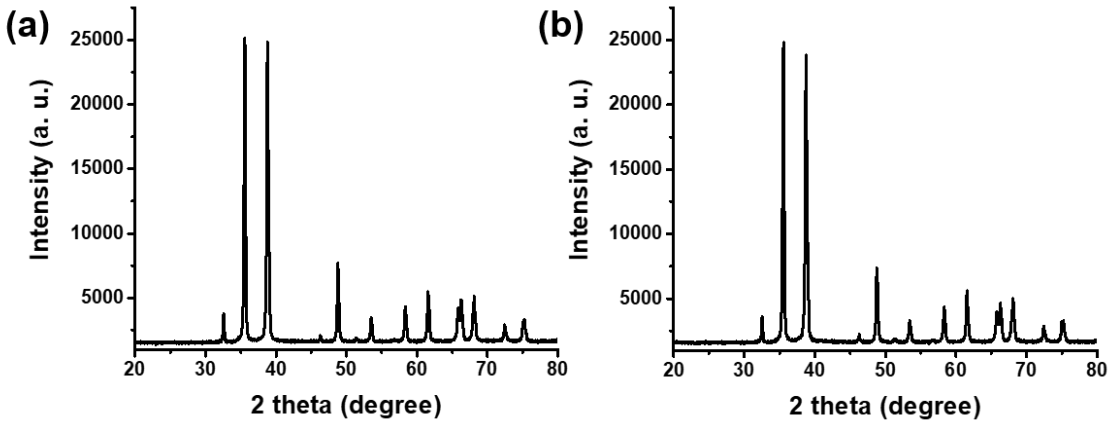

Fig. S7. XRD pattern of (a) CuO and (b) Pd/CuO.

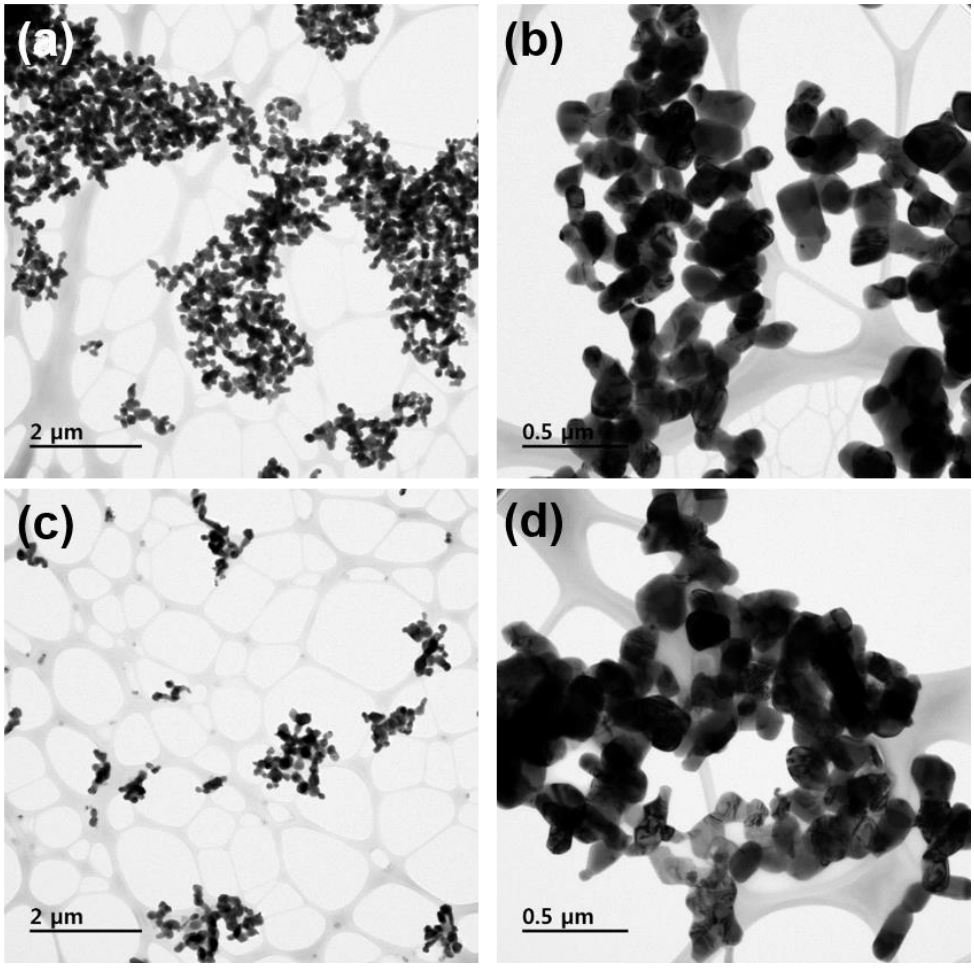

Fig. S8. TEM image of Pd/CuO (a) and (b). TEM image of CuO (c) and (d).

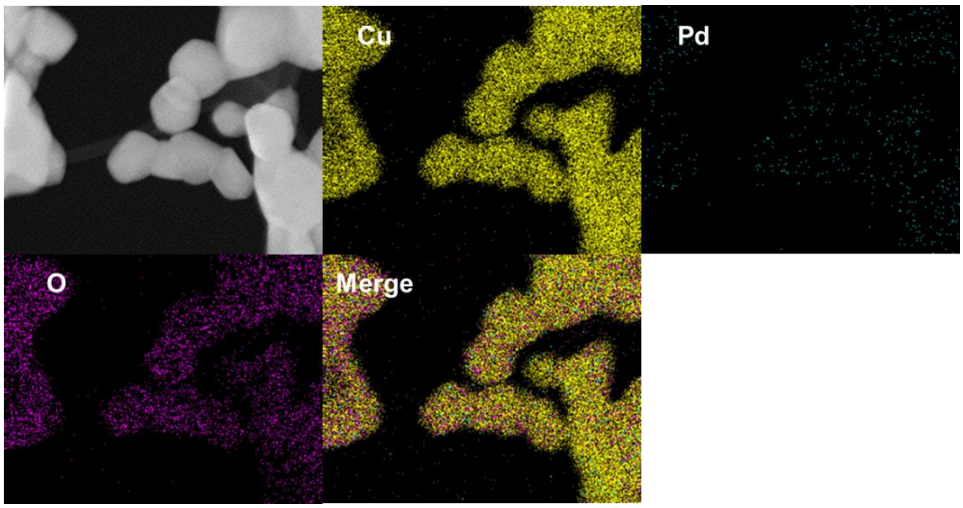

Fig. S9. HAADF-STEM and elemental maping image of Pd/CuO.

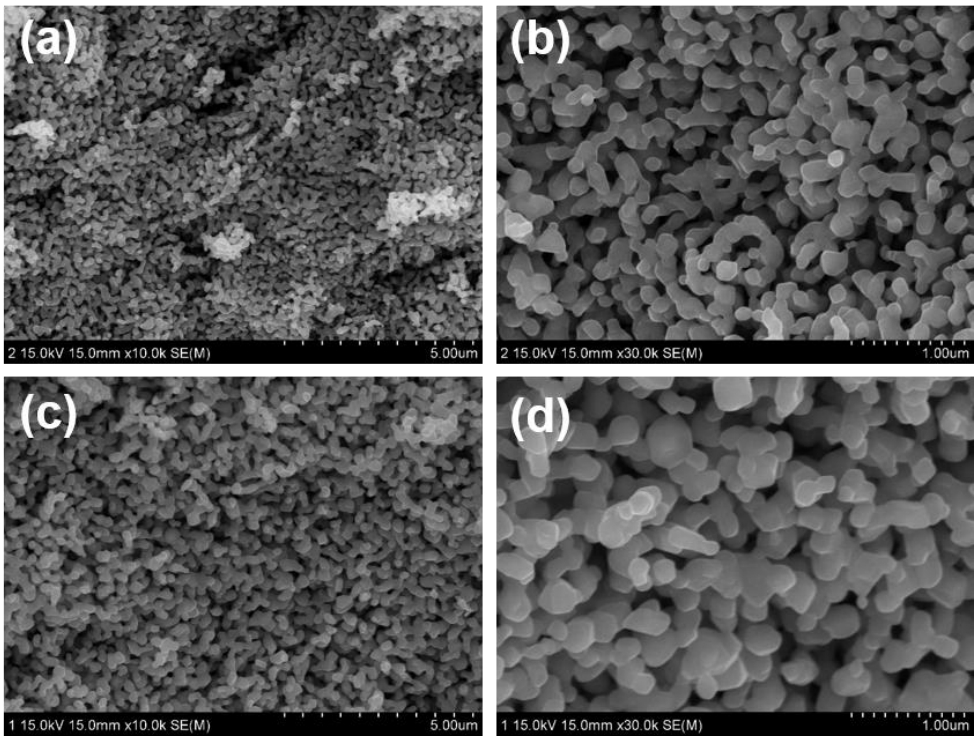

Fig. S10. SEM image of Pd/CuO (a) and (b). SEM image of CuO (c) and (d).

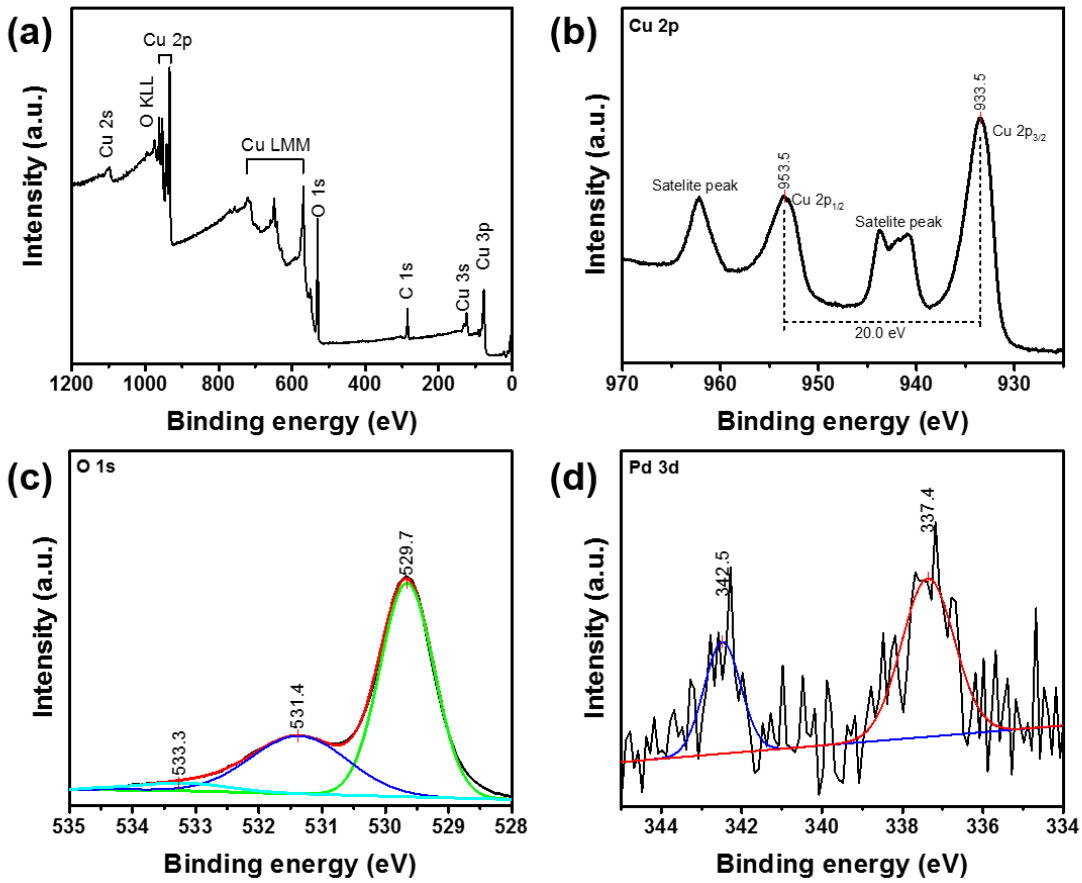

Fig. S11. XPS spectra of Pd/CuO. (a) survey XPS spectrum. (b) High-resolution XPS spectrum of Cu 2p. (C) High-resolution XPS spectra of O 1s. (d) High-resolution XPS spectra of Pd 3d.

XPS analysis was used to investigate the surface composition and valence states of the Pd/CuO. The XPS spectra of the Pd/CuO are presented in Fig. S10. As shown in Fig. S10 (b), the peaks at 933.5 and 953.5 eV were assigned to Cu $2p_{3/2}$ and Cu 2p1/2 of Cu^{2+} in CuO, respectively [14,15]. Also, there were clear satellite peaks located at higher binding energies to Cu 2p. These peaks are typically indicative of the existence of Cu^{2+} in CuO [16]. The O 1s region showed three peaks at 529.7, 531.4, and 533.3 eV, which are attributed to the O in CuO, O-H bond of the hydroxyl group, and adsorbed water molecules, respectively [17,18]. These results were same with the XPS analysis of CuO (Fig. S11). Fig. S10 (d) shows high-resolution XPS spectra of Pd 3d. The two peaks

located at 337.4 and 342.5 eV were assigned to Pd $3d_{5/2}$ and Pd $3d_{3/2}$ [19]. These Pd 3d binding energy of Pd/CuO were higher than the Pd 3d binding energy of PdO and metallic Pd [20]. Previously, positive chemical shift of Pd 3d have been observed in Pd^{2+} located in solid solution [21,22]. Similar with that, the high Pd 3d binding energy of Pd/CuO can be come from the change of environmental of Pd^{2+} in CuO.

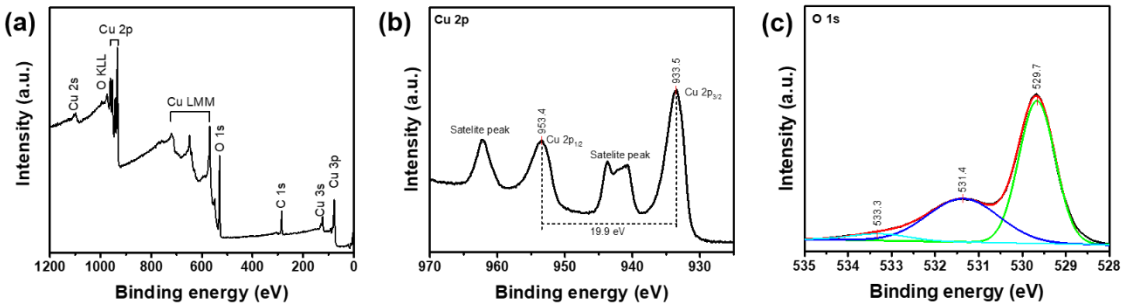

Fig. S12. XPS spectra of CuO. (a) survey XPS spectrum. (b) High-resolution XPS spectrum of Cu 2p. (C) High-resolution XPS spectra of O 1s.

Characterization table

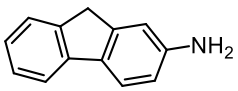

9*H*-fluoren-2-amine (**2a**)

After the general procedures, the crude was purified by column chromatography (eluent: ethyl acetate/Hex = 1:3) to give **2a** as a yellowish solid (0.0855 g, 94%). ^{1}H NMR (400 MHz, $CDCl_3$) δ 7.65 (d, *J* = 7.6 Hz, 1H), 7.58 (d, *J* = 7.9 Hz, 1H), 7.48 (d, *J* = 7.3 Hz, 1H), 7.33 (t, *J* = 7.0 Hz, 1H), 7.21 (td, *J* = 7.4, 1.0 Hz, 1H), 6.88 (s, 1H), 6.72 (dd, *J* = 7.9, 2.1 Hz, 1H), 3.82 (s, 2H), 3.71 (s, 2H). ^{13}C NMR (100 MHz, $CDCl_3$) δ 145.8, 145.3, 142.4, 142.2, 133.1, 126.7, 125.2, 124.9, 120.8, 118.7, 114.1, 111.9, 36.9. The NMR data were consistent with the reported data.[23]

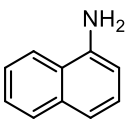

Naphthalen-1-amine (**2b**)

After the general procedures, the crude was purified by column chromatography (eluent: ethyl acetate/Hex = 1:6) to give **2b** as a brownish solid (0.0666 g, 93%). ^{1}H NMR (400 MHz, $CDCl_3$) δ 7.79–7.85 (m, 2H), 7.45–7.49 (m, 2H), 7.28–7.34 (m, 2H), 6.79 (dd, *J* = 6.9, 1.6 Hz, 1H), 4.15 (s, 2H). ^{13}C NMR (100 MHz, $CDCl_3$) δ 142.1, 134.5, 128.6, 126.4, 125.9, 125.0, 123.8, 120.6, 119.1, 109.8. The NMR data were consistent with the reported data.[24]

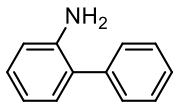

[1,1'-biphenyl]-2-amine (**2c**)

After the general procedures, the crude was purified by column chromatography (eluent: ethyl acetate/Hex = 1:6) to give **2c** as a brownish solid (0.0616 g, 73%). ^{1}H NMR (400 MHz, $CDCl_3$) δ 7.42–7.47 (m, 4H), 7.32–7.38 (m, 1H), 7.16 (qd, *J* = 7.6, 1.6 Hz, 2H), 6.85 (td, *J* = 7.4, 1.1 Hz, 1H), 6.80 (dd, *J* = 7.9, 1.0 Hz, 1H), 3.87 (s, 2H). ^{13}C NMR (100 MHz, $CDCl_3$) δ 143.0, 139.5, 130.6, 129.2, 128.9, 128.6, 128.1, 127.3, 119.2, 116.0. The NMR data were consistent with the reported data.[23]

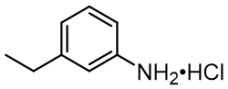

3-ethylaniline hydrochloride (**2d·HCl**)

After the general procedures, the crude was purified by column chromatography (eluent: ethyl acetate/Hex = 1:3) and HCl bubbling to give **2d·HCl** as a gray solid (0.0491 g, 62%). ^{1}H NMR (400 MHz, DMSO-d_6) δ 10.41 (s, 3H), 7.38 (t, *J* = 7.8 Hz, 1H), 7.22 (q, *J* = 7.9 Hz, 3H), 2.63 (q, *J* = 7.5 Hz, 2H), 1.17 (t, *J* = 7.6 Hz, 3H). ^{13}C NMR (100 MHz, DMSO-d_6) δ 146.1, 132.6, 130.1, 127.9, 122.8, 121.0, 28.4, 15.9. The NMR data were consistent with the **2d·HCl** portion of the reported data.[25]

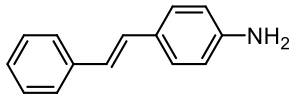

(*E*)-4-styrylaniline (**2e**)

After the general procedures, the crude was purified by column chromatography (eluent: ethyl acetate/Hex = 1:6) to give **2e** as a yellowish solid (0.0842 g, 86%). ^{1}H NMR (400 MHz, DMSO-d_6) δ 7.49 (d, *J* = 8.5 Hz, 2H), 7.26–7.34 (m, 4H), 7.15–7.20 (m, 1H), 6.97 (dd, *J* = 68.3, 16.4 Hz, 2H), 6.54–6.57 (m, 2H), 5.30 (s, 2H). ^{13}C NMR (100 MHz, DMSO-d_6) δ 149.3, 138.5, 129.6, 129.1, 128.2, 127.0, 126.3, 125.2, 123.3, 114.4. The NMR data were consistent with reported data.[26]

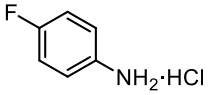

4-Fluoroaniline hydrochloride (**2f·HCl**)

After the general procedures, the crude was purified by column chromatography (eluent: ethyl acetate/Hex = 1:3). The column purified product was dissolved in organic solvent and bubbled with HCl (g) to give **2f·HCl** as a white solid (0.0496 g, 68%). ^{1}H NMR (400 MHz, DMSO-d_6) δ 10.37 (s, 2H), 7.41–7.46 (m, 2H), 7.30–7.36 (m, 2H). ^{13}C NMR (100 MHz, DMSO-d_6) δ 161.5 (d, *J* = 244.4), 129.2 (d, *J* = 2.9 Hz), 125.7 (d, *J* = 8.6 Hz), 117.1 (d, *J* = 23 Hz). The NMR data were consistent with reported data.[27]

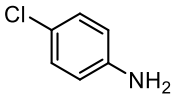

4-Chloroaniline (**2g**)

After the general procedures, the crude was purified by column chromatography (eluent: ethyl acetate/Hex = 1:5) to give **2g** as a yellow solid (0.0450 g, 71%). ^{1}H NMR (400 MHz, $CDCl_3$) δ 7.10 (td, *J* = 6.0, 3.5 Hz, 2H), 6.61 (td, *J* = 6.0, 3.5 Hz, 2H), 3.65 (s, 2H). ^{13}C NMR (100 MHz, $CDCl_3$) δ 145.1, 129.3, 123.3, 116.4. The NMR data were consistent with reported data.[23]

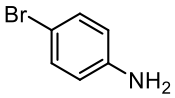

4-Bromoaniline (**2h**)

After the general procedures, the crude was purified by column chromatography (eluent: ethyl acetate/Hex = 1:4) to give **2h** as a white solid (0.0525 g, 61%). ^{1}H NMR (400 MHz, $CDCl_3$) δ 7.23 (dt, *J* = 9.4, 2.6 Hz, 2H), 6.56 (dt, *J* = 9.4, 2.6 Hz, 2H), 3.66 (s, 2H). ^{13}C NMR (100 MHz, $CDCl_3$) δ 145.5, 132.1, 116.8, 110.3. The NMR data were consistent with reported data.[28]

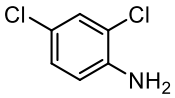

2,4-Dichloroaniline (**2i**)

After the general procedures, the crude was purified by column chromatography (eluent: ethyl acetate/Hex = 1:4) to give **2i** as a white solid (0.0650 g, 80%). ^{1}H NMR (400 MHz, $CDCl_3$) δ 7.23 (d, *J* = 2.3 Hz, 1H), 7.02 (dd, *J* = 8.5, 2.3 Hz, 1H), 6.67 (d, *J* = 8.7 Hz, 1H), 4.02 (s, 2H). ^{13}C NMR (100 MHz, $CDCl_3$) δ 141.7, 129.0, 127.8, 122.9, 119.7, 116.4. The NMR data were consistent with reported data.[29]

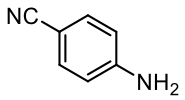

4-Aminobenzonitrile (**2j**)

After the general procedures, the crude was purified by column chromatography (eluent: ethyl acetate/Hex = 1:3) to give **2j** as a brownish solid (0.0615 g, 53%). ^{1}H NMR (400 MHz, DMSO-d_6) δ 7.38 (dt, *J* = 9.0, 2.1 Hz, 2H), 6.60 (dt, *J* = 9.0, 2.3 Hz, 2H), 6.13 (s, 2H). ^{13}C NMR (100 MHz, DMSO-d_6) δ 153.0, 133.4, 120.7, 113.4, 95.5. The NMR data were consistent with reported data.[26]

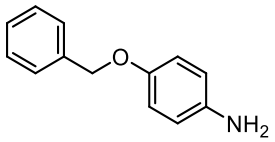

4-(Benzyloxy)aniline (**2k**)

After the general procedures, the crude was purified by column chromatography (eluent: ethyl acetate/Hex = 1:3) to give **2k** as a brownish solid (0.0315 g, 98%). ^{1}H NMR (400 MHz, $CDCl_3$) δ 7.31–7.45 (m, 5H), 6.84 (td, *J* = 6.2, 3.8 Hz, 2H), 6.65 (td, *J* = 6.2, 3.8 Hz, 2H), 5.01 (s, 2H), 3.23 (s, 2H). ^{13}C NMR (100 MHz, $CDCl_3$) δ 152.1, 140.3, 137.6, 128.6, 128.0, 127.6, 116.5, 116.2, 70.9. The NMR data were consistent with reported data.[28]

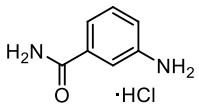

3-Aminobenzamide hydrochloride (**2l·HCl**)

After the general procedures, the crude was purified by column chromatography (eluent: ethyl acetate/Hex = 1:3). The column purified product was dissolved in organic solvent and bubbled with HCl (g) to give **2l·HCl** as a white solid (0.0758 g, 88%). ^{1}H NMR (400 MHz, DMSO-d_6) δ 10.20 (s, 2H), 8.14 (s, 1H), 7.87 (d, *J* = 7.3 Hz, 1H), 7.82 (s, 1H), 7.50–7.56 (m, 3H). ^{13}C NMR (101 MHz, DMSO-d_6) δ 167.3, 136.3, 133.6, 130.2, 126.5, 126.0, 122.8.

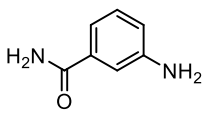

3-Aminobenzamide (**2l**)

After the base work-up of **2l·HCl**, **2l** was obtained as a white solid and analyzed by NMR. ^{1}H NMR (400 MHz, DMSO-d_6) δ 7.73 (s, 1H), 7.14 (s, 1H), 7.03–7.07 (m, 2H), 6.97 (dt, *J* = 7.5, 1.3 Hz, 1H), 6.67 (dq, *J* = 7.9, 1.1 Hz, 1H), 5.19 (s, 2H). ^{13}C NMR (100 MHz,

DMSO-d_6) δ 169.2, 149.1, 135.7, 129.2, 117.0, 115.2, 113.6. The NMR data were consistent with reported data.[30]

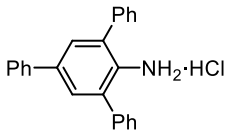

5'-Phenyl-[1,1':3',1''-terphenyl]-2'-amine hydrochloride (**2m·HCl**)

After the general procedures, the crude was purified by column chromatography (eluent: ethyl acetate/Hex = 1:20). The column purified product was dissolved in organic solvent and bubbled with HCl (g) to give **2m·HCl** as a white solid (0.1425 g, 80%). ^{1}H NMR (400 MHz, DMSO-d_6) δ 7.68 (dd, *J* = 15.7, 7.2 Hz, 6H), 7.53 (t, *J* = 7.5 Hz, 4H), 7.40–7.46 (m, 6H), 7.31 (t, *J* = 7.5 Hz, 1H), 6.61 (s, 3H). ^{13}C NMR (100 MHz, DMSO-d_6) δ 139.3, 137.9, 137.1, 135.1, 130.2, 130.0, 129.3, 129.2, 128.9, 128.4, 127.8, 127.0.

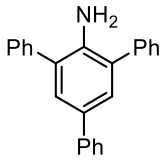

5'-Phenyl-[1,1':3',1''-terphenyl]-2'-amine (**2m**)

After the base work-up of **2m·HCl**, **2m** was obtained and analyzed by NMR. ^{1}H NMR (400 MHz, $CDCl_3$) δ 7.57–7.62 (m, 6H), 7.50 (t, *J* = 7.5 Hz, 4H), 7.38–7.43 (m, 6H), 7.26–7.31 (m, 1H). ^{13}C NMR (100 MHz, $CDCl_3$) δ 140.9, 140.1, 139.7, 131.4, 129.5, 129.1, 128.8, 128.6, 128.5, 127.6, 126.6, 126.5. The NMR data were consistent with reported data.[31]

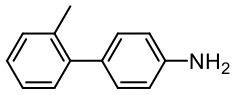

2'-methyl-[1,1'-biphenyl]-4-amine (**2n**)

After the one-pot reaction, the crude was purified by column chromatography (eluent: hexane to ethyl acetate/Hex = 1:20) to give **2n** as a yellow oil (0.0750 g, 82%). ^{1}H NMR (400 MHz, $CDCl_3$) δ 7.22–7.27 (m, 4H), 7.14 (dt, *J* = 8.9, 2.3 Hz, 2H), 6.74 (dt, *J* = 8.8, 2.3 Hz, 2H), 3.70 (s, 2H), 2.30 (s, 3H). ^{13}C NMR (100 MHz, $CDCl_3$) δ 145.3, 142.0, 135.6, 132.3, 130.4, 130.2, 130.0, 126.8, 125.8, 114.8, 20.7. The NMR data were consistent with reported data.[32]

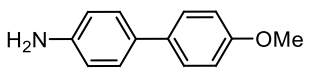

4'-Methoxy-[1,1'-biphenyl]-4-amine (**2o**)

After the one-pot reaction, the crude was purified by column chromatography (eluent:

ethyl acetate/Hex = 1:3) to give **2o** as a yellow solid (0.0689 g, 69%). ^{1}H NMR (400 MHz, $CDCl_3$) δ 7.46 (d, *J* = 8.7 Hz, 2H), 7.37 (d, *J* = 8.5 Hz, 2H), 6.95 (d, *J* = 8.9 Hz, 2H), 6.75 (d, *J* = 8.7 Hz, 2H), 3.84 (s, 3H), 3.70 (s, 2H). ^{13}C NMR (100 MHz, $CDCl_3$) δ 158.5, 145.4, 134.0, 131.5, 127.7, 127.5, 115.5, 114.2, 55.4. The NMR data were consistent with reported data.[33]

Table S2. Comparison for the reduction of nitroarenes.[a]

Catalyst	Amount of catalyst	Reaction condition	time	yield (%)	Reference
Pd/CuO	0.005 mol% Pd 5 mol% Cu	$NaBH_4$ (3 equiv) EtOH/H_2O (1:1), 40 °C	0.5–40 h	13 examples (53–98)	This work
Fe/ppm Pd + Ni NPs	0.008 mol% Pd 0.16 mol% Ni 2 mol% Fe	NaBH4 (3 equiv) 2 wt% TPGS-750-M/H_2O, 10% THF, rt	15 min–16 h	27 examples (74–99)	34
Pd cNPs/C@Fe_3O_4	0.73 mol% Pd	Hydrazine hydrate (3 equiv) EtOH, 70 °C	1 h	12 examples 96–99	35
Pd/g-C_3N_4	1 mol% Pd	Formic acid (3 equiv) H_2O, 25 °C	5–120 min	12 examples 92–99	19
$Fe(OTf)_3$	10 mol% Fe	$NaBH_4$ (20 equiv) EtOH, rt	4 h	25 examples 33–95 (24–80)	36
MRN-Pd	1 mol% Pd	$NaBH_4$ (1.2 equiv) H_2O, rt	45 min	11 examples 83–99	37
AgNCs	5 mol% Ag	$NaBH_4$ (10 equiv) H_2O, rt	0.5–6 h	12 examples (71–97)	38
Pd@CTF	1 mol% Pd	Formic acid (5 equiv) NH_3CO_2H (5 equiv) EtOH/H_2O (4:1), rt	0.33–2.5 h	14 examples 91–99	39
Cu/SiO_2@$NiFe_2O_4$	2.6 mol% Cu	$NaBH_4$ (10 equiv) MeOH/H_2O (1:1)	12–210 min	11 examples 59–100	40

[a]The yield in parentheses is the isolated yield.

Calculation of simple E factor (sEF) using Table 2. Entry 1.[41, 42]

Recently, a simpler E factor (sEF) was proposed by Roschangar and co-workers.[41] The sEF consist of raw materials, reagents, and product. The sEF value of table 2. entry 1

was calculated, and calculated sEF was 0.92. This value will help in the process development of this reaction.

$$\text{sEF} = \frac{\sum \text{m(Raw materials)} + \sum \text{m(Reagents)} - \text{m(Product)}}{\text{m(Product)}}$$

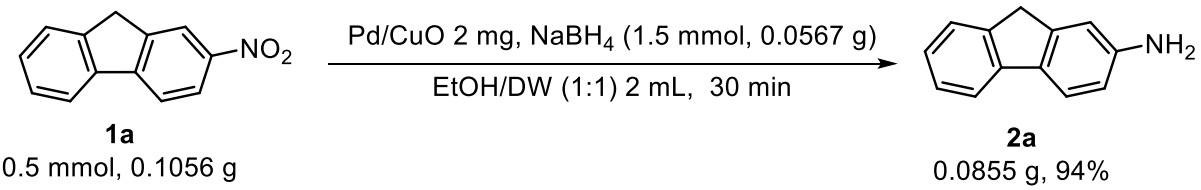

1a
0.5 mmol, 0.1056 g

2a
0.0855 g, 94%

sEF = 0.92

References

[1] Tai, C. Y.; Tai, C.-T.; Chang, M.-H.; Liu, H.-S. *Ind. Eng. Chem. Res.* **2007**, *46*, 5536–5541.

[2] Yue, W.; Zhou, W. *J. Mater. Chem.* **2007**, *17*, 4947–4952.

[3] Yang, G.; Yan, W.; Wang, J.; Yang, H. *CrystEngComm* **2014**, *16*, 6907–6913.

[4] Fageria, P.; Gangopadhyay, S.; Pande, S. *RSC adv.* **2014**, *4*, 24962–24971.

[5] Gangwar, J.; Gupta, B. K.; Tripathi, S. K.; Srivastava, A. K. *Nanoscale* **2015**, *7*, 13313–13344.

[6] Lu, P.; Hu, X.; Li, Y.; Zhang, M.; Liu, X.; He, Y.; Dong, F.; Fu, M.; Zhang, Z. *RSC Adv.* **2018**, *8*, 6315–6325.

[7] Gao, Y.; Chen, K.; Tan, X.; Wang, X.; Alsaedi, A.; Hayay, T.; Chen, C. *ACS Sustainable Chem. Eng.* **2017**, *5*, 2163–2171.

[8] Hossain, S. T.; Mukherjee, S. K. *Langmuir* **2012**, *28*, 16614–16622.

[9] Huang, B.; Zhang, Z.; Zhao, C.; Cairang, L.; Bai, J.; Zhang, Y.; Mu, X.; Du, J.; Wang, H.; Pan, X.; Zhou, J.; Xie, E. *Sens. Actuators B* **2018**, *255*, 2248–2257.

[10] Selvan, R. K.; Perelshtein, I.; Perkas, N.; Gedanken, A. *J. Phys. Chem. C.* **2008**, *112*, 1825–1830.

[11] Molinder, R.; Comyn, T. P.; Hondow, N.; Parker, J. E.; Dupont, V. *Energy Environ. Sci.* **2012**, *5*, 8958–8969.

[12] Jadhav, A. P.; Pawar, A. U.; Pal, U.; Kang, Y. S. *J. Mater. Chem. C* **2014**, *2*, 496–500.

[13] Xu, L.; Zhang, J.; Li, Z.; Ma, Q.; Wang, Y.; Cui, F.; Gui, T. *New J. Chem.* **2019**, *43*, 520–526.

[14] Dubale, A. A.; Pan, C.-J.; Tamirat, A. G.; Chen, H.-M.; Su, W.-N.; Chen, C.-H.; Rick, J.; Ayele, D. W.; Aragaw, B. A.; Lee, J.-F.; Yang, Y.-W.; Hwang, B.-J. *J. Mater. Chem. A* **2015**, *3*, 12482–12499.

[15] He, D.; Wang, G.; Liu, G.; Suo, H.; Zhao, C. *Dalton Trans.* **2017**, *46*, 3318–3324.

[16] Wang, G.; Sui, Y.; Zhang, M.; Xu, M.; Zeng, Q.; Liu, C.; Liu, X.; Du, F.; Zou, B. *J. Mater. Chem. A* **2017**, *5*, 18577–18584.

[17] Xu, X.; Gao, Z.; Cui, Z.; Liang, Y.; Li, Z.; Zhu, S.; Yang, X.; Ma, J. *ACS Appl. Mater. Interfaces* **2016**, 8, 91–101.

[18] Fu, W.; Cao, Y.; Feng, Q.; Smith, W. R.; Dong, P.; Ye, M.; Shen, J. *Nanoscale* **2019**, *11*, 1379–1385.

[19] Xu, X.; Luo, J.; Li, L.; Zhang, D.; Wang, Y.; Li, G. *Green Chem.* **2018**, *20,* 2038–2046.

[20] Zhao, M.; Li, X.; Zhang, L.; Zhang, C.; Gong, M.; Chen, Y. *Catal. Today* **2011**, *175,* 430–434.

[21] Gulyaev, R. V.; Stadnichenko, A. I.; Slavinskaya, E. M.; Ivanova, A. S.; Koscheev, S. V.; Boronin, A. I. *Appl. Catal. A* **2012**, *439–440,* 41–50.

[22] Christensen, G. L.; Langell, M. A. *J. Phys. Chem. C* **2013**, *117,* 7039–7049.

[23] García, N.; García-García, P.; Fernández-Rodríguez, M. A.; Rubio, R.; Pedrosa, M. R.; Arnáiz, F. J.; Sanz, R. *Adv. Synth. Catal.* 2012, *354*, 321–327.

[24] Yang, S.-T.; Shen, P.; Liao, B.-S.; Liu, Y.-H.; Peng, S.-M.; Liu, S.-T. *Organometallics* 2017, *36*, 3110–3116.

[25] de Noronha, R. G.; Romão, C. C.; Fernandes, A. C. *J. Org. Chem.* 2009, *74*, 6960–6964.

[26] Gholinejad, M.; Oftadeh, E.; Shojafar, M.; Sansano, J.; Lipshutz, B. H. *ChemSusChem* 2019, *12*, 4240–4248.

[27] Lenstra, D. C.; Wolf, J. J.; Mecinović, J. *J. Org. Chem.* 2019, *84*, 6536–6545.

[28] Orlandi, M.; Tosi, F.; Bonsignore, M.; Benaglia, M. *Org. Lett.* 2015, *17*, 3941–3943.

[29] Kale, A.; Medishetti, N.; Kanugala, S.; C, G. K.; Atmakur, K. *Org. Biomol. Chem.* 2019, *17*, 3186–3194.

[30] Rahaim Jr., R. J.; Maleczka Jr, R. E. *Org. Lett.* 2005, *7*, 5087–5090.

[31] Bolliger, J. L.; Frech, C. M. *Adv. Synth. Catal.* 2010, *352*, 1075–1080.

[32] Chahdoura, F.; Pradel, C.; Gómez, M. *Adv. Synth. Catal.* 2013, *355*, 3648–3660.

[33] Razler, T. M.; Hsiao, Y.; Qian, F.; Fu, R.; Khan, R. K.; Doubleday, W. *J. Org. Chem.*

2009, *74*, 1381–1384.

[34] Pang, H.; Gallou, F.; Sohn, H.; Camacho-Bunquin, J.; Delferro, M.; Lipshutz, B. H. *Green Chem.* **2018**, *20*, 130–135.

[35] Kumar, B. S.; Amali, A. J.; Pitchumani, K. *J. Mol. Catal. A: Chem.* **2016**, *423*, 511–519.

[36] MacNair, A. J.; Tran, M.-M.; Nelson, J. E.; Sloan, G. U.; Ironmonger, A.; Thomas, S. P. *Org. Biomol. Chem.* **2014**, *12*, 5082–5088.

[37] Shokouhimehr, M.; Hong, K.; Lee, T. H.; Moon, C. W.; Hong, S. P.; Zhang, K.; Suh, J. M.; Choi, K. S.; Varma, R. S.; Jang, H. W. *Green Chem.* **2018**, *20*, 3809–3817.

[38] Giri, S.; Das, R.; van der Westhuyzen, C.; Maity, A. *Appl. Catal., B.* **2017**, *209*, 669–678.

[39] Li, J.; Zhang, L.; Liu, X; Shang, N.; Gao, S.; Feng, C.; Wang, C.; Wang, Z. *New J. Chem.* **2018**, *42*, 9684–9689.

[40] Parmekar, M. V.; Salker, A. V. *RSC Adv.* **2016**, *6*, 108458–108467.

[41] Roschangar, R.; Sheldon, R. A.; Senanayake, C. H. *Green Chem.* **2015**, *17*, 752–762.

[42] Degtyareva, E. S.; Borkovskaya, E. V.; Ananikov, V. P. *ACS Sustainable Chem. Eng.* **2019**, *7*, 9680–9689.

Spectral copies of ^{1}H NMR and ^{13}C NMR

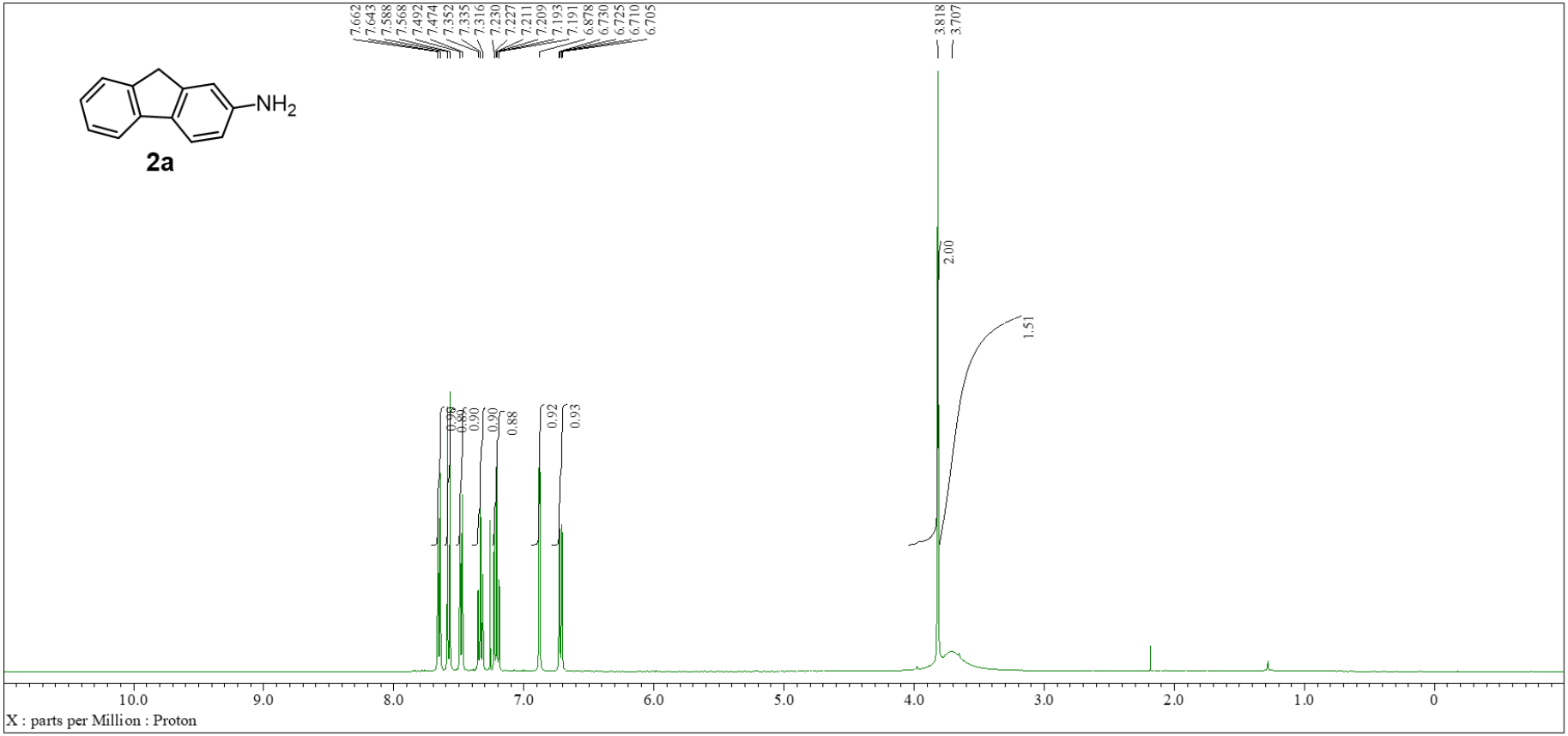

^{1}H NMR of **2a**

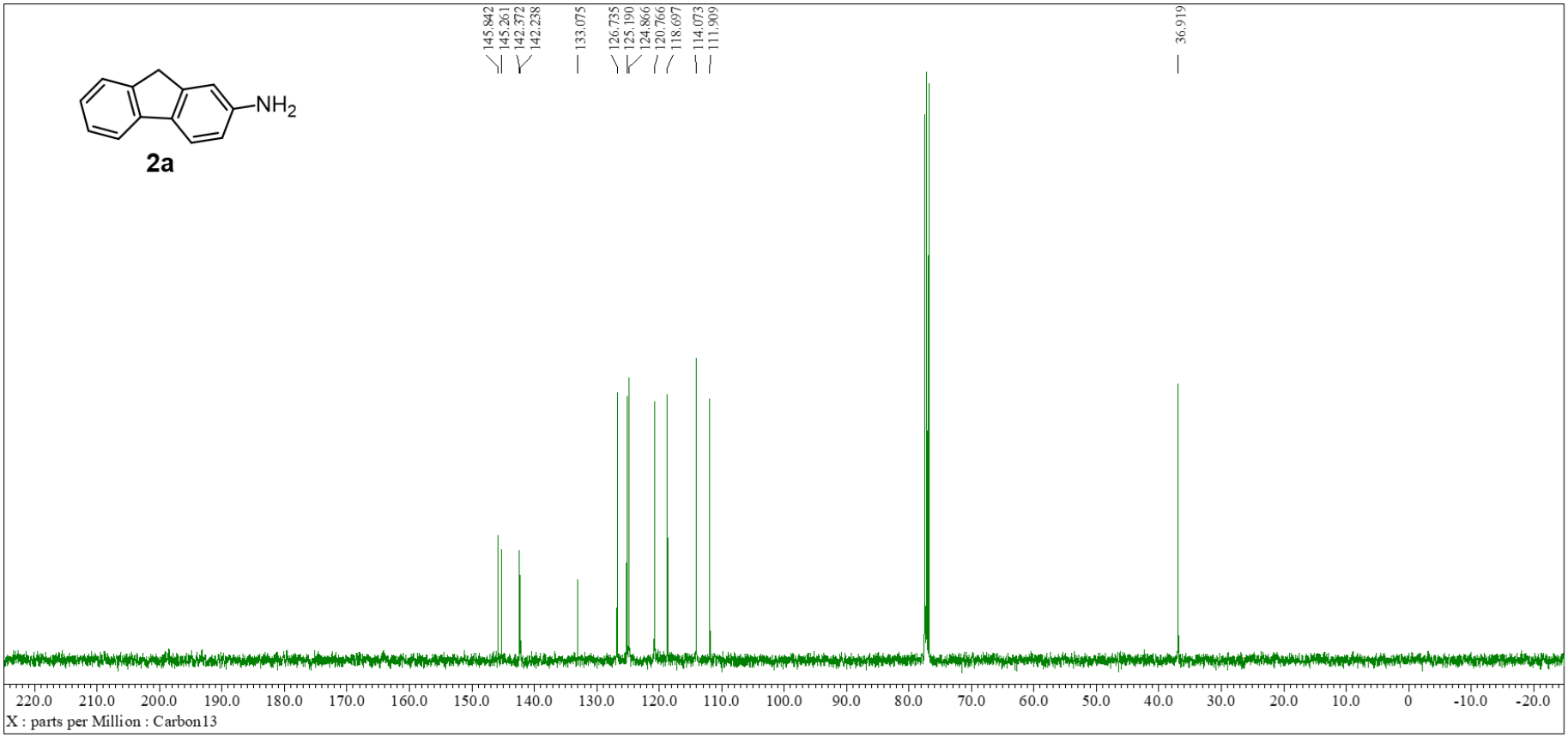
145.842
145.261
142.372
142.238
133.075
126.735
125.190
124.866
120.766
118.697
114.073
111.909
36.919
NH2
2a
220.0 210.0 200.0 190.0 180.0 170.0 160.0 150.0 140.0 130.0 120.0 110.0 100.0 90.0 80.0 70.0 60.0 50.0 40.0 30.0 20.0 10.0 0 -10.0 -20.0
X : parts per Million : Carbon13

^{13}C NMR of **2a**

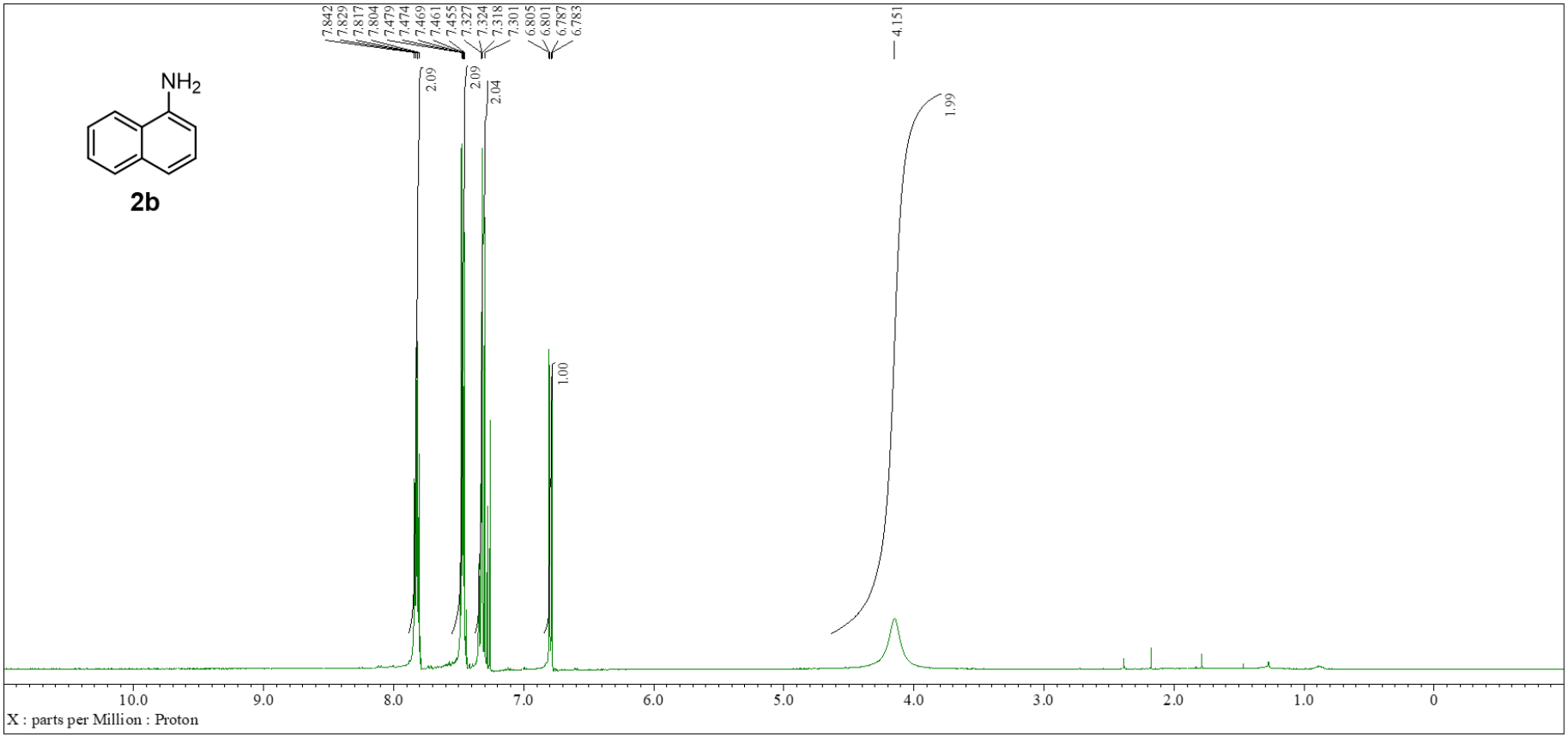
7.842
7.829
7.817
7.804
7.479
7.474
7.469
7.461
7.455
7.327
7.324
7.318
7.301
6.805
6.801
6.787
6.783
4.151
2.09
2.09
2.04
1.99
1.00
NH2
2b
10.0
9.0
8.0
7.0
6.0
5.0
4.0
3.0
2.0
1.0
0
X : parts per Million : Proton

^{1}H NMR of **2b**

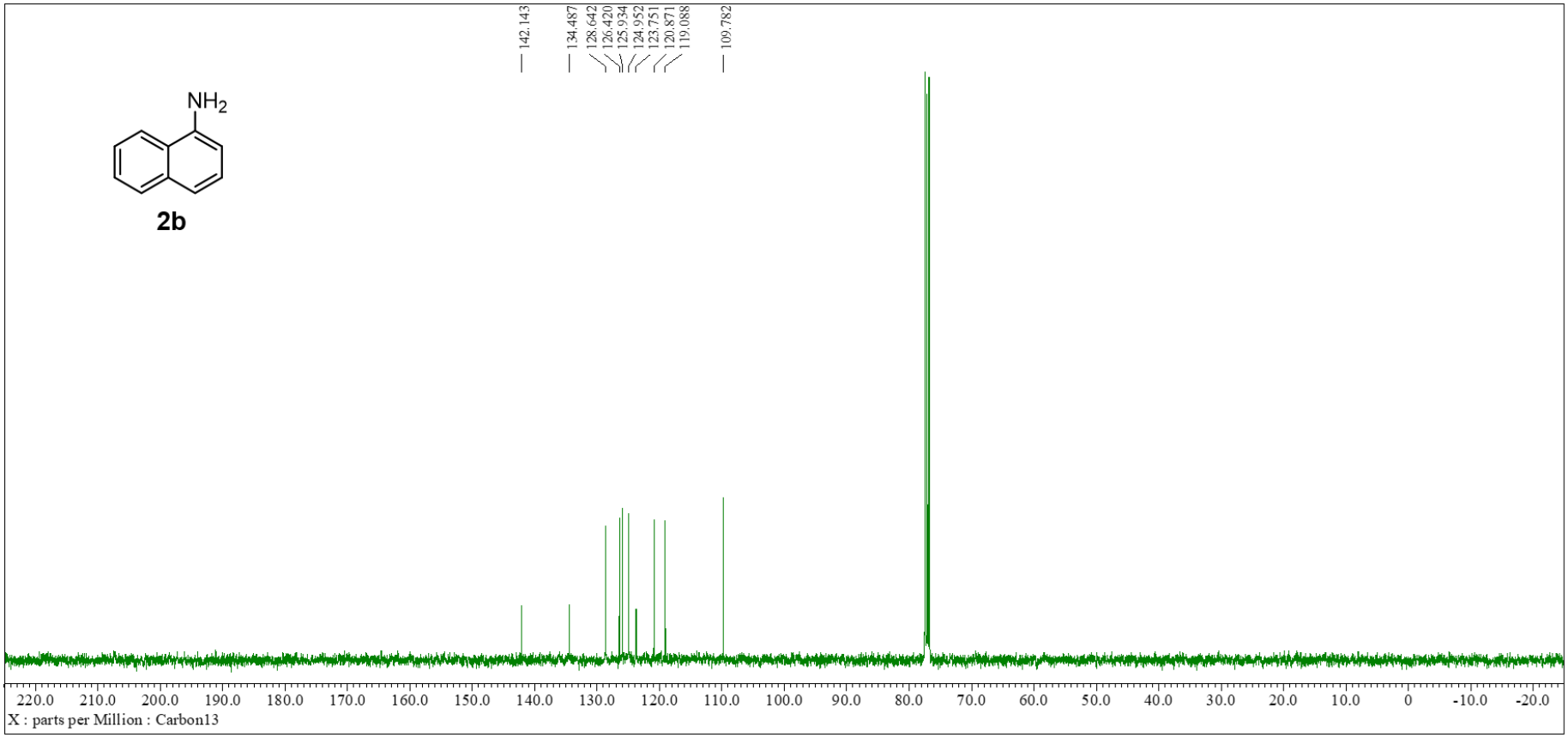
142.143
134.487
128.642
126.420
125.934
124.952
123.751
120.871
119.088
109.782
NH2
2b
220.0 210.0 200.0 190.0 180.0 170.0 160.0 150.0 140.0 130.0 120.0 110.0 100.0 90.0 80.0 70.0 60.0 50.0 40.0 30.0 20.0 10.0 0 -10.0 -20.0
X : parts per Million : Carbon13

^{13}C NMR of **2b**

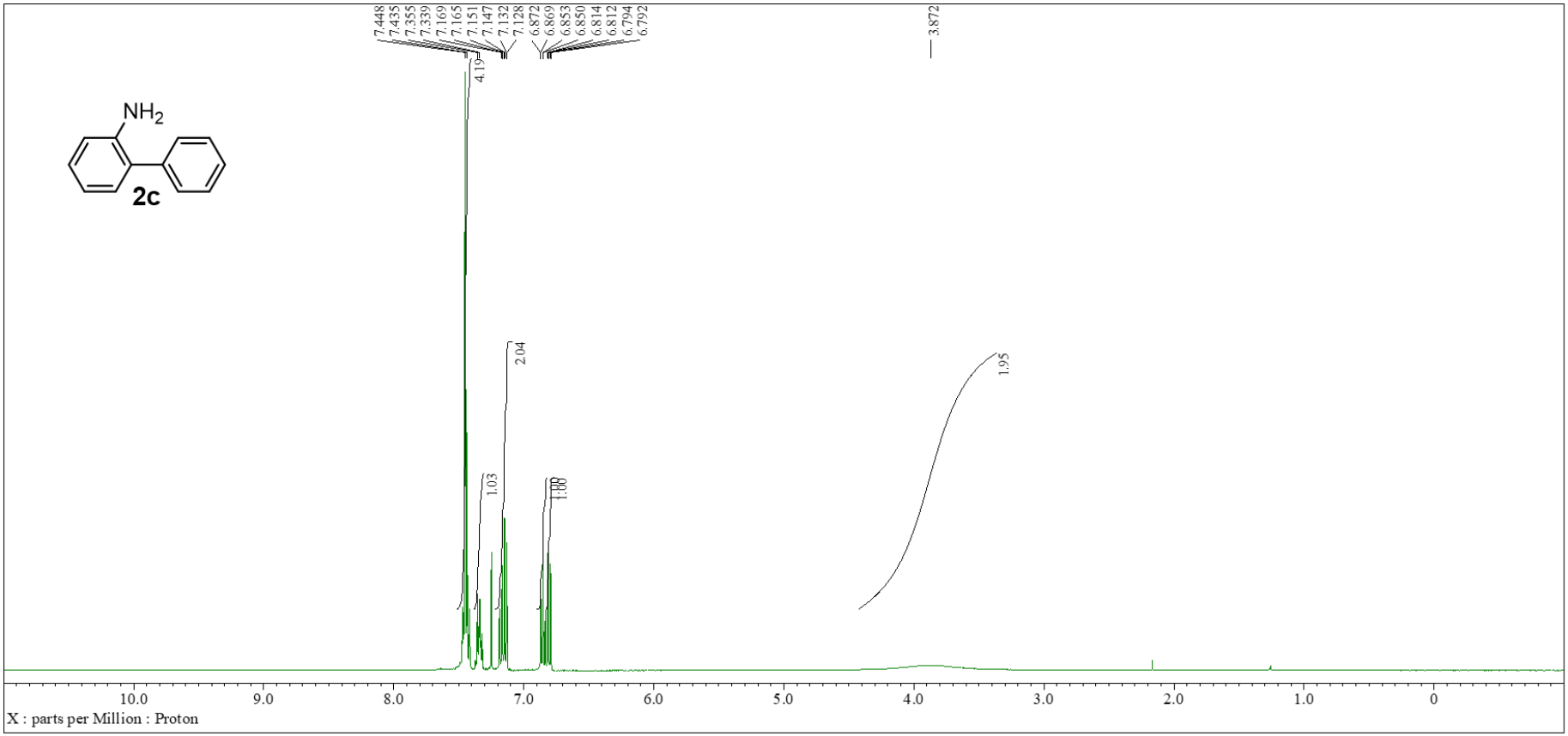
7.448
7.435
7.355
7.339
7.169
7.165
7.151
7.147
7.132
7.128
6.872
6.869
6.853
6.850
6.814
6.812
6.794
6.792
3.872
4.19
2.04
1.95
1.03
1.00
1.00
NH2
2c
10.0
9.0
8.0
7.0
6.0
5.0
4.0
3.0
2.0
1.0
0
X : parts per Million : Proton

^{1}H NMR of **2c**

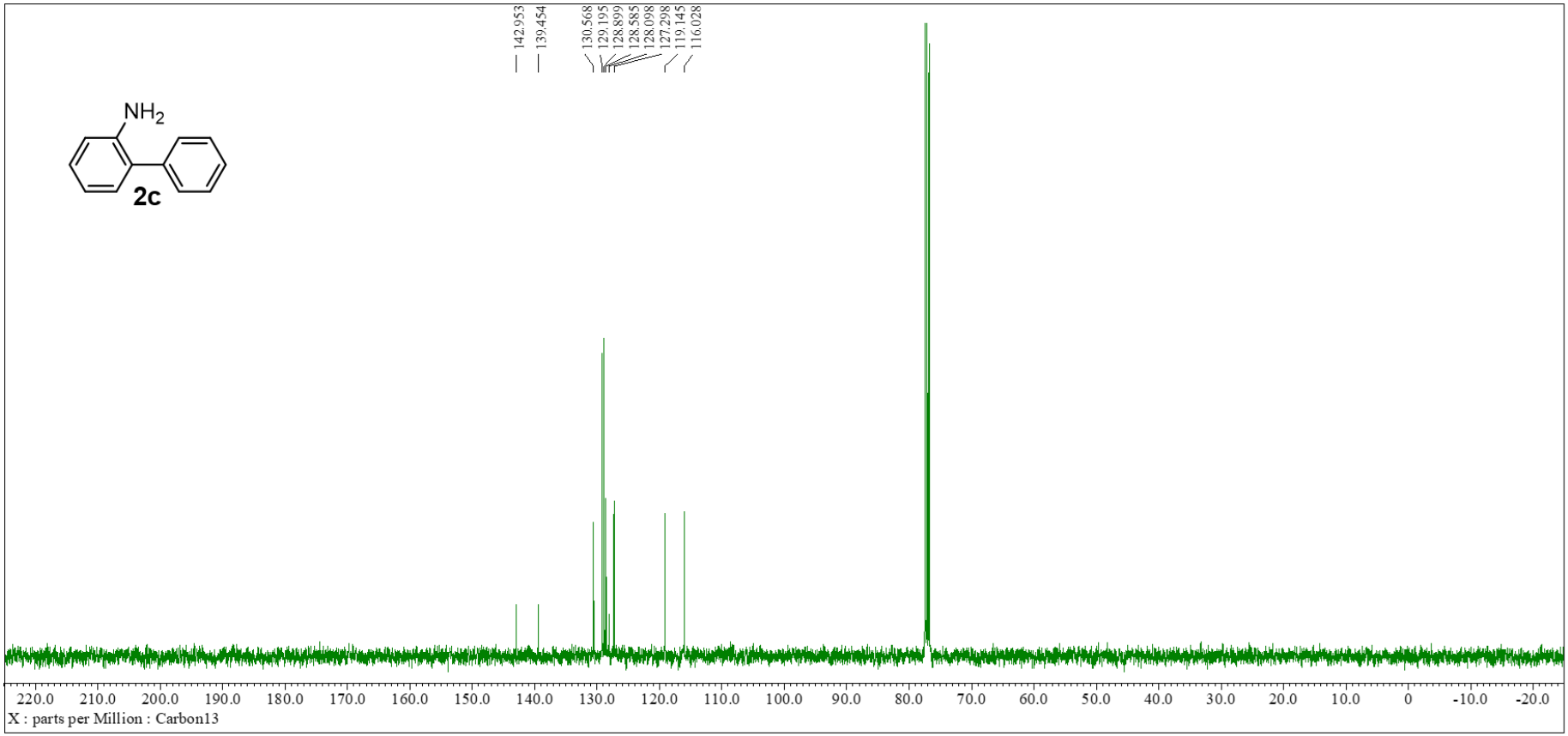
142.953
139.454
130.568
129.195
128.899
128.585
128.098
127.298
119.145
116.028
NH2
2c
220.0 210.0 200.0 190.0 180.0 170.0 160.0 150.0 140.0 130.0 120.0 110.0 100.0 90.0 80.0 70.0 60.0 50.0 40.0 30.0 20.0 10.0 0 -10.0 -20.0
X : parts per Million : Carbon13

^{13}C NMR of **2c**

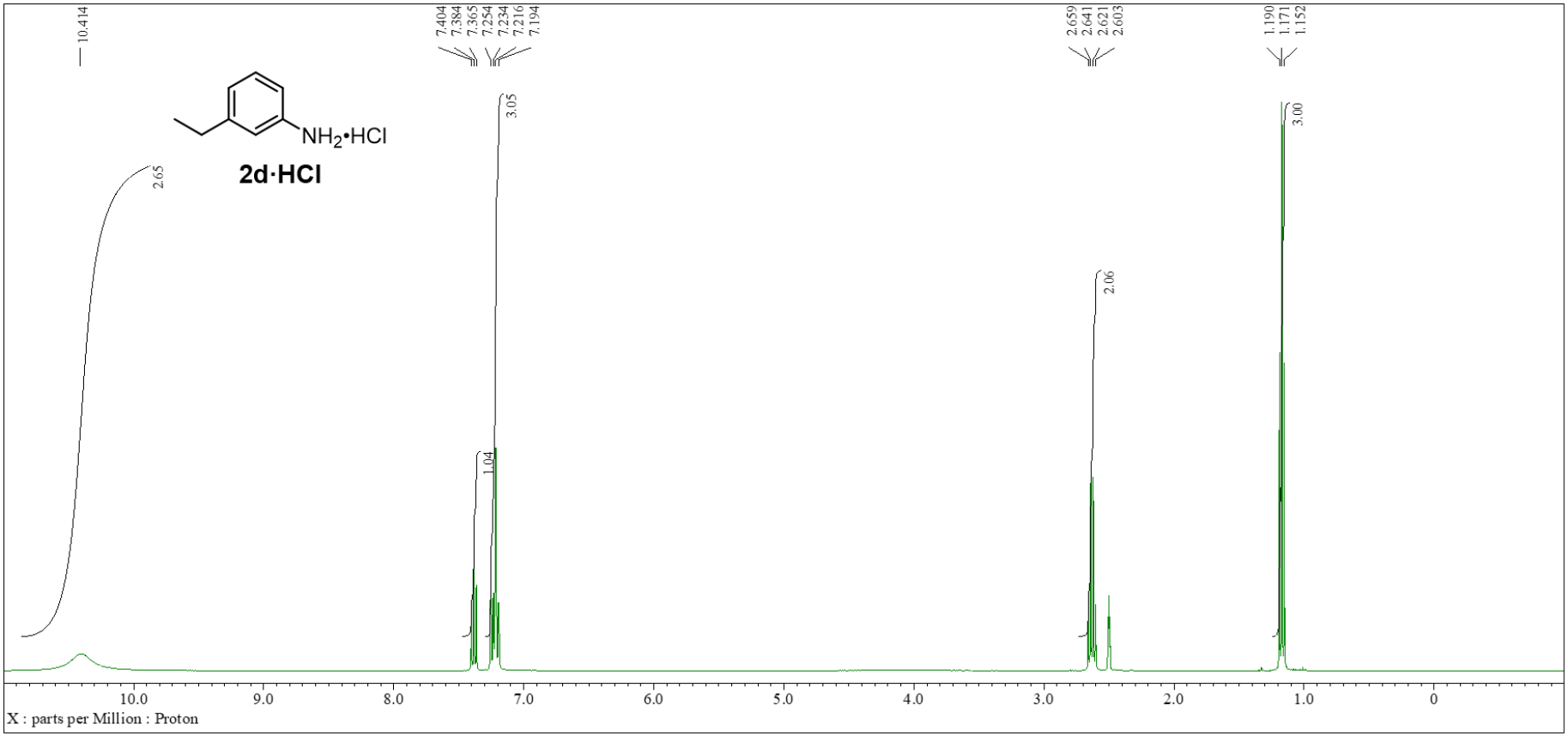

^{1}H NMR of **2d·HCl**

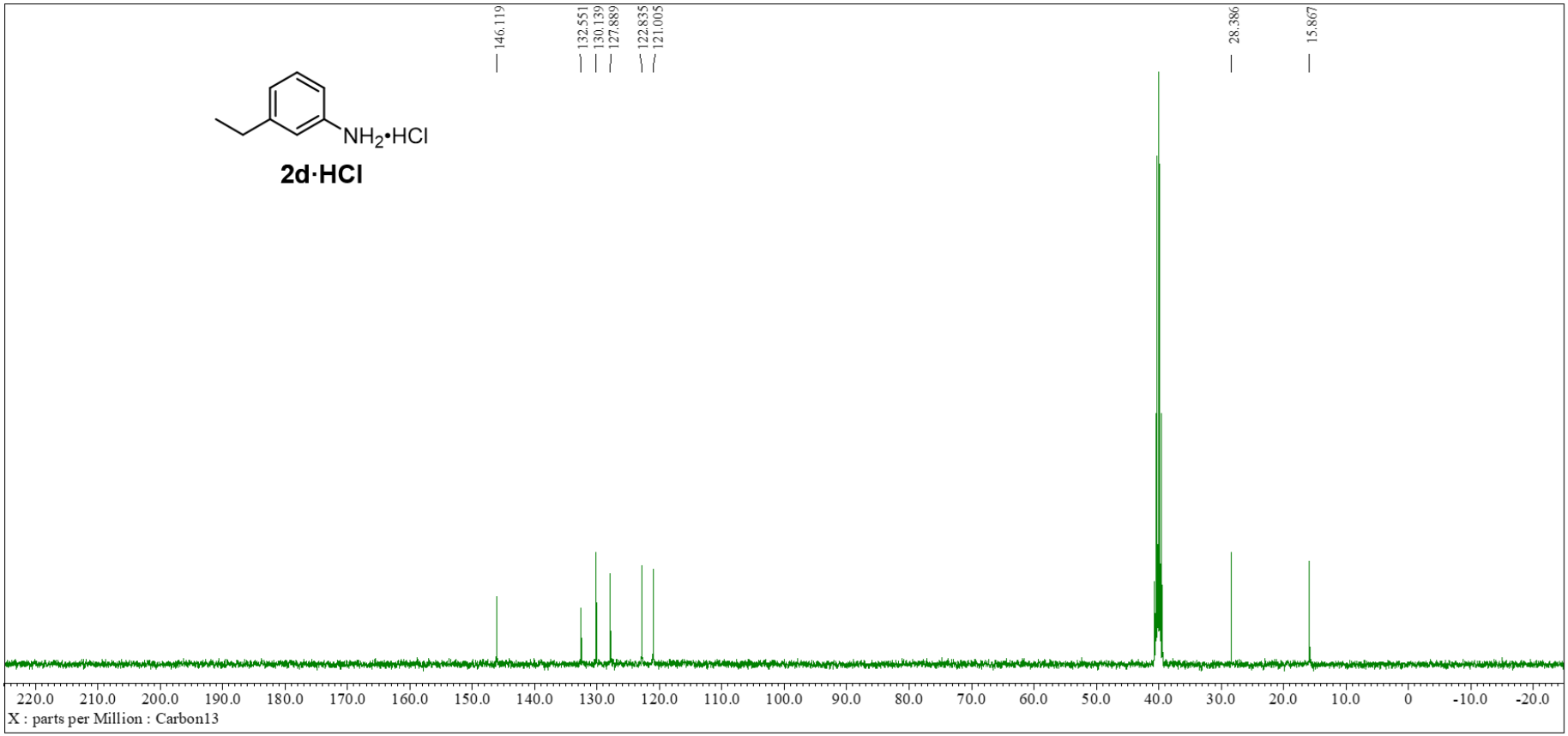

^{13}C NMR of **2d·HCl**

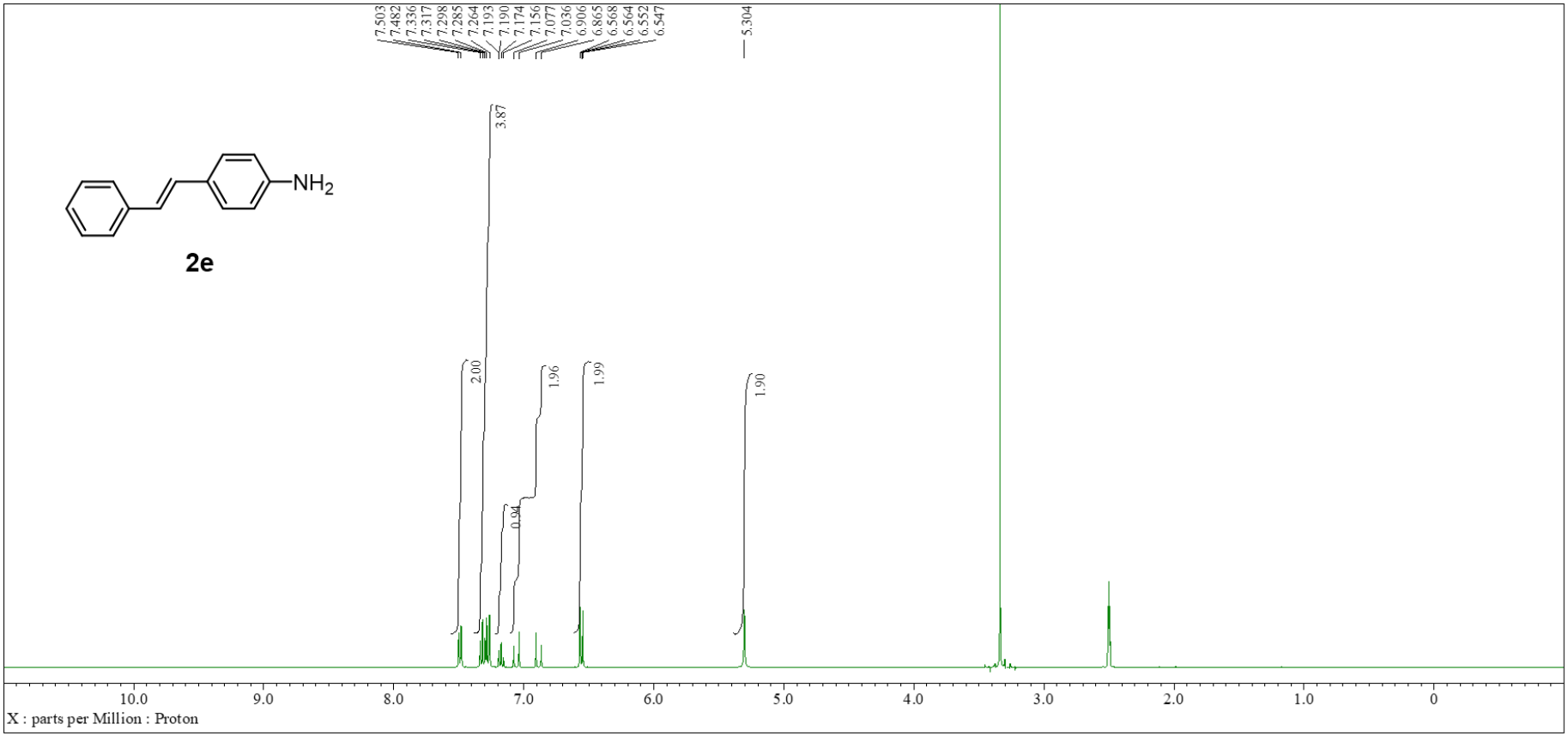
7.503
7.482
7.336
7.317
7.298
7.285
7.264
7.193
7.190
7.174
7.156
7.077
7.036
6.906
6.865
6.568
6.564
6.552
6.547
5.304
3.87
2.00
1.96
1.99
1.90
0.94
NH2
2e
10.0
9.0
8.0
7.0
6.0
5.0
4.0
3.0
2.0
1.0
0
X : parts per Million : Proton

^{1}H NMR of **2e**

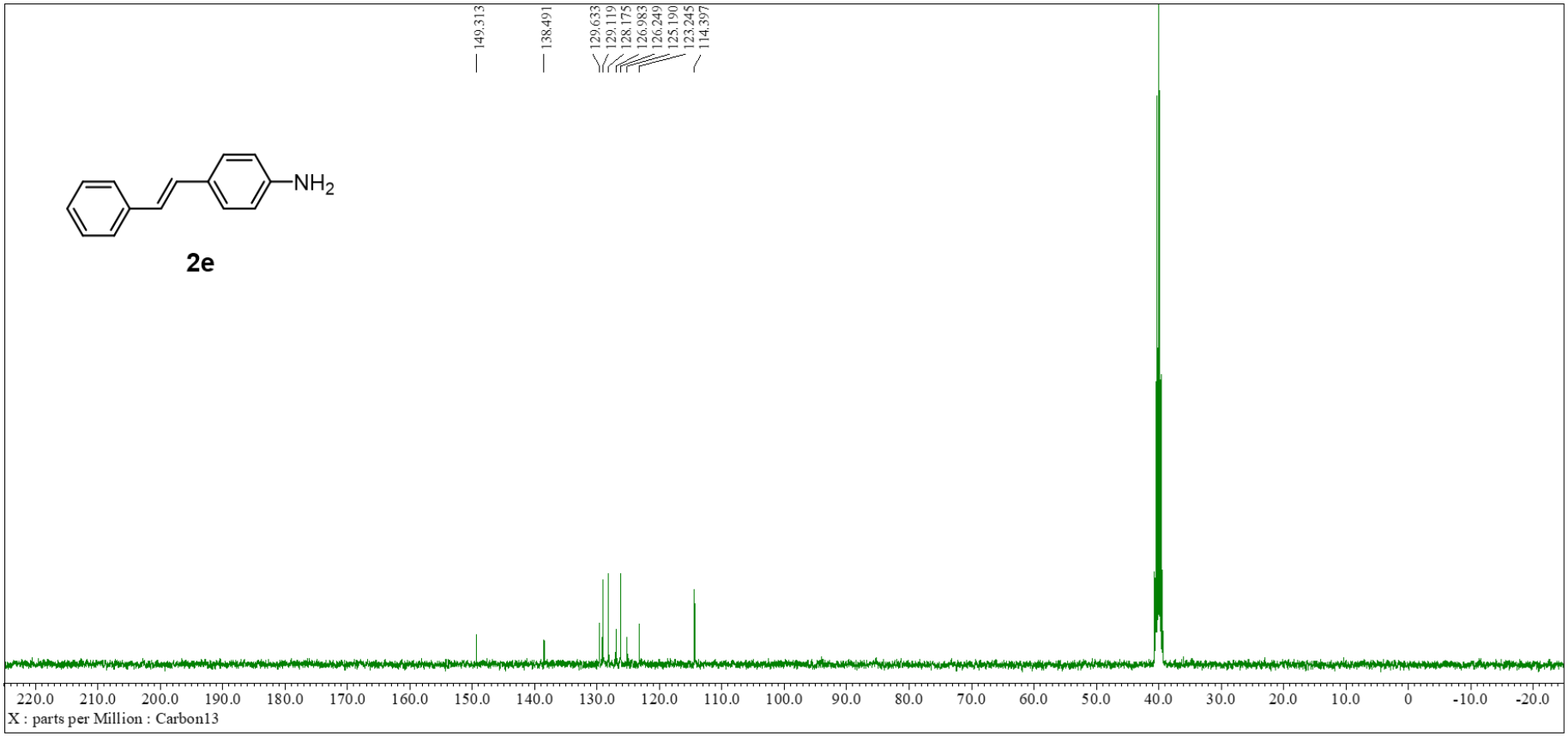
149.313
138.491
129.633
129.119
128.175
126.983
126.249
125.190
123.245
114.397
NH2
2e
220.0 210.0 200.0 190.0 180.0 170.0 160.0 150.0 140.0 130.0 120.0 110.0 100.0 90.0 80.0 70.0 60.0 50.0 40.0 30.0 20.0 10.0 0 -10.0 -20.0
X : parts per Million : Carbon13

^{13}C NMR of **2e**

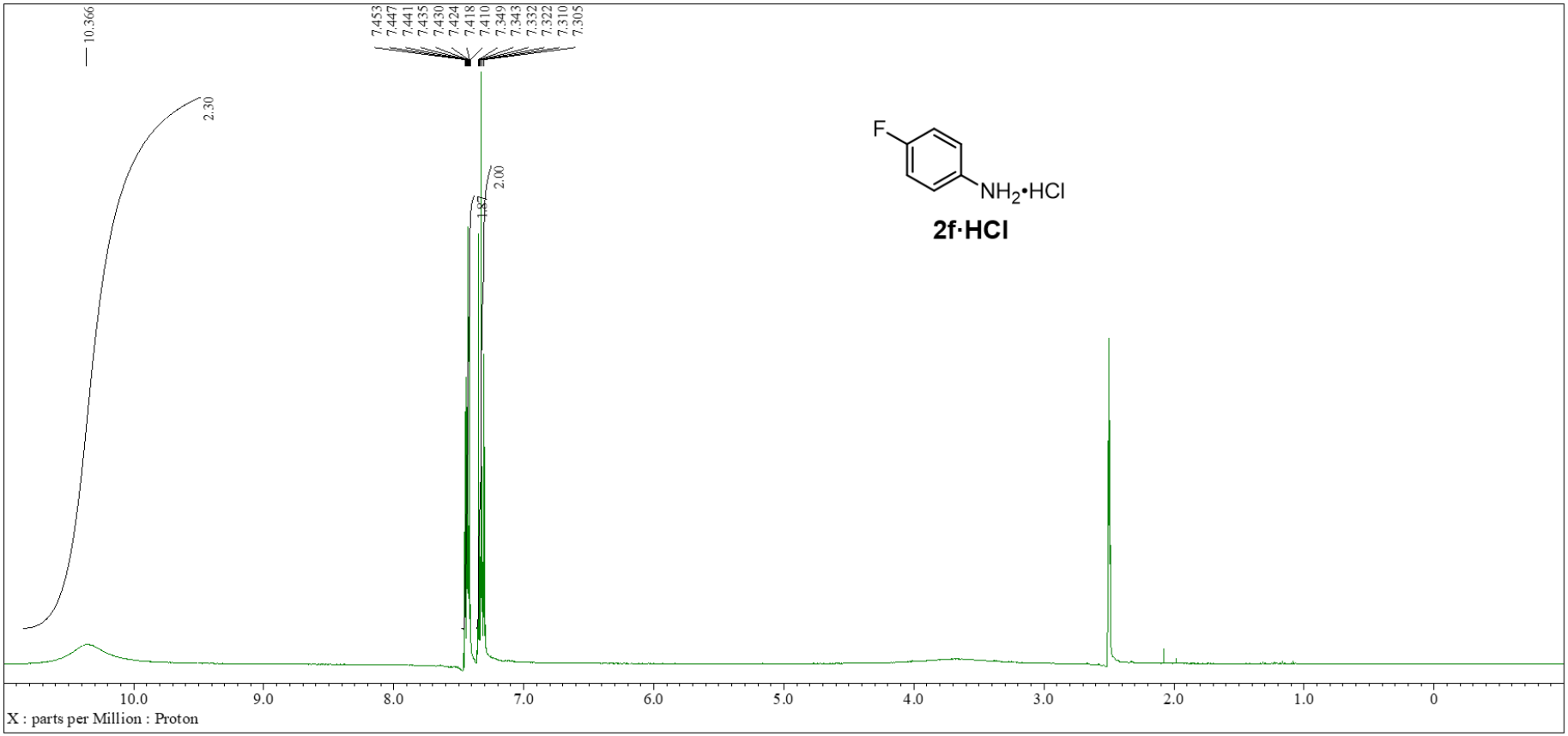

^{1}H NMR of **2f·HCl**

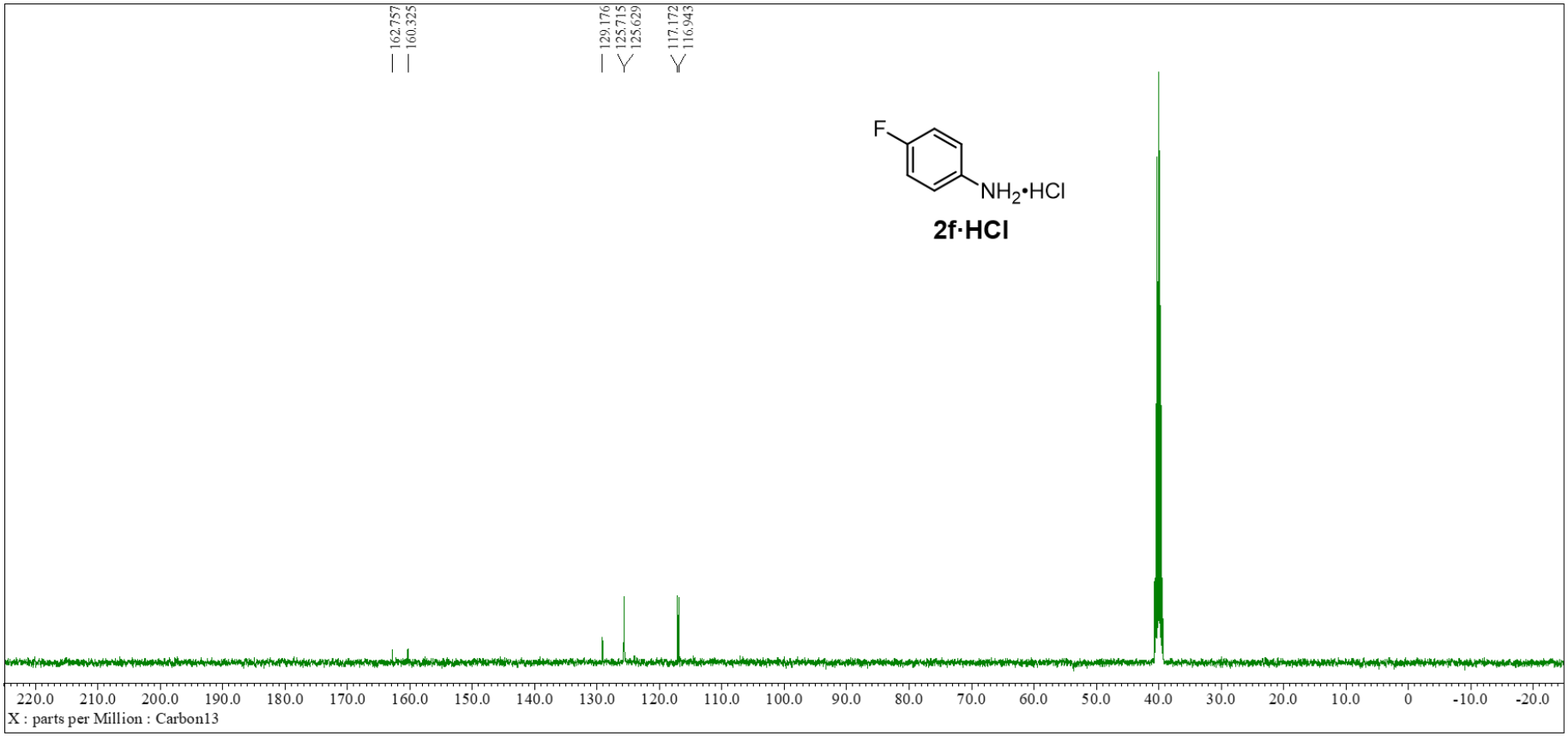

^{13}C NMR of **2f·HCl**

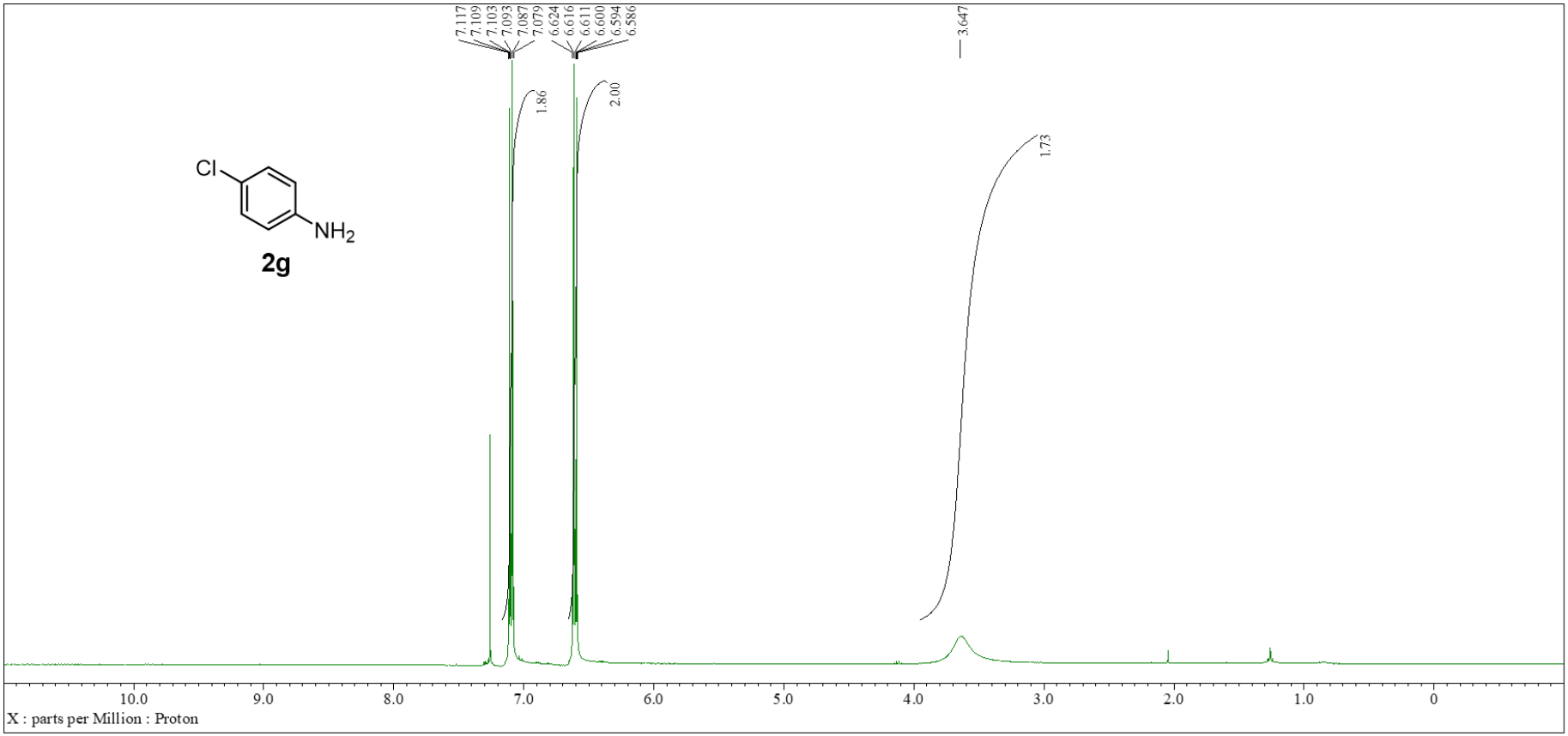
7.117
7.109
7.103
7.093
7.087
7.079
6.624
6.616
6.611
6.600
6.594
6.586
3.647
1.86
2.00
1.73
Cl
NH2
2g
10.0
9.0
8.0
7.0
6.0
5.0
4.0
3.0
2.0
1.0
0
X : parts per Million : Proton

^{1}H NMR of **2g**

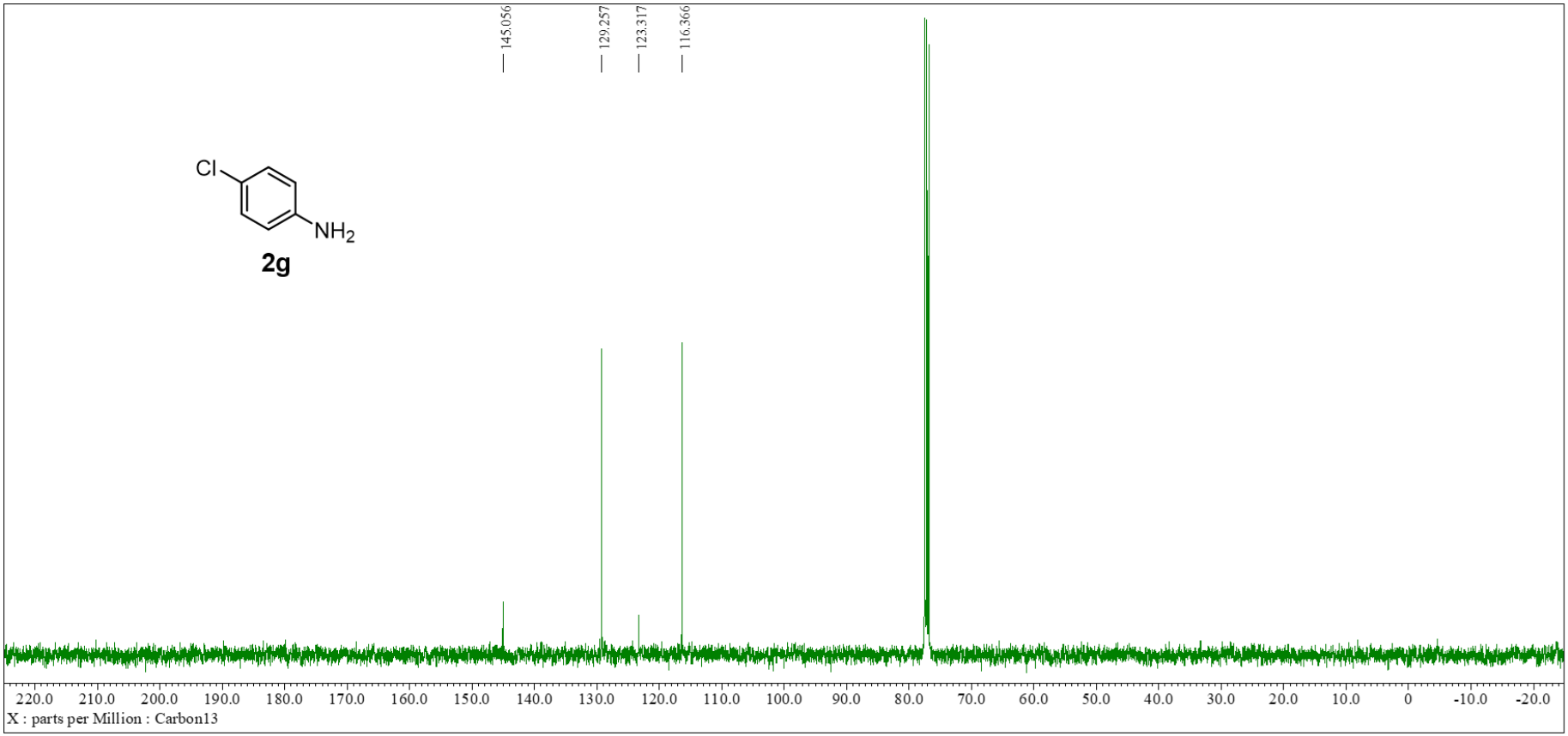
145.056
129.257
123.317
116.366
Cl
NH2
2g
220.0 210.0 200.0 190.0 180.0 170.0 160.0 150.0 140.0 130.0 120.0 110.0 100.0 90.0 80.0 70.0 60.0 50.0 40.0 30.0 20.0 10.0 0 -10.0 -20.0
X : parts per Million : Carbon13

^{13}C NMR of **2g**

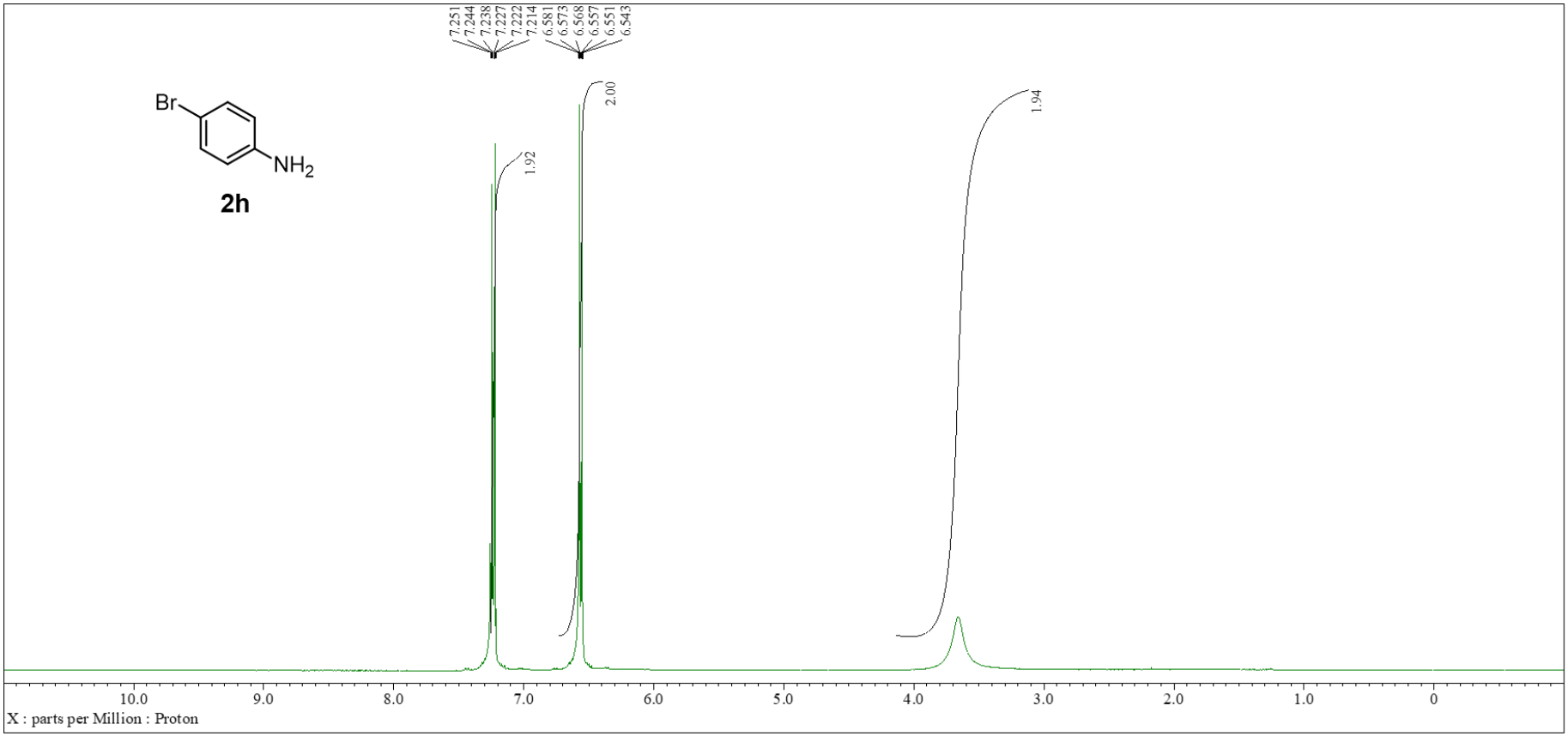
7.251
7.244
7.238
7.227
7.222
7.214
6.581
6.573
6.568
6.557
6.551
6.543
Br
NH2
2h
1.92
2.00
1.94
10.0
9.0
8.0
7.0
6.0
5.0
4.0
3.0
2.0
1.0
0
X : parts per Million : Proton

^{1}H NMR of **2h**

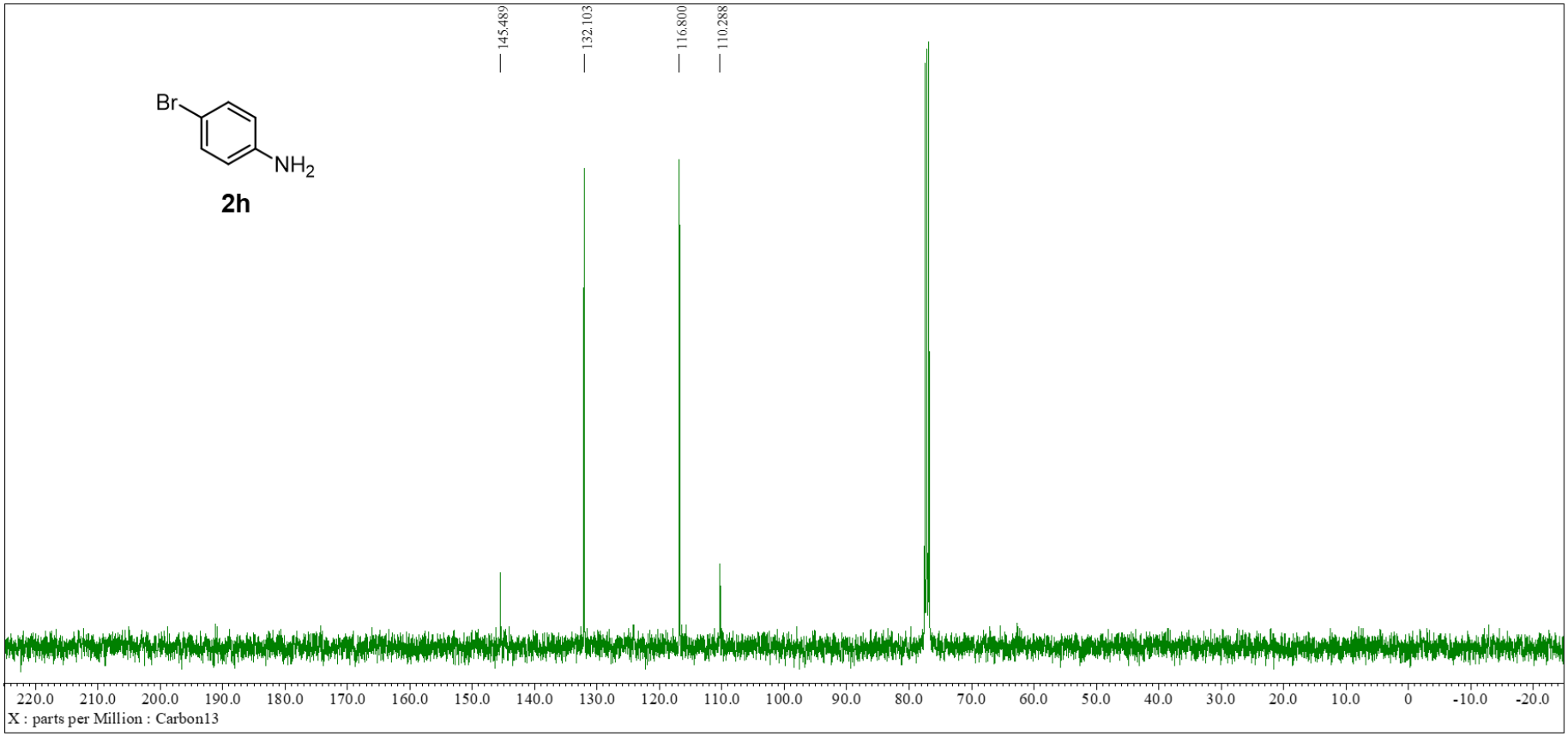
145.489
132.103
116.800
110.288
Br
NH2
2h
220.0 210.0 200.0 190.0 180.0 170.0 160.0 150.0 140.0 130.0 120.0 110.0 100.0 90.0 80.0 70.0 60.0 50.0 40.0 30.0 20.0 10.0 0 -10.0 -20.0
X : parts per Million : Carbon13

^{13}C NMR of **2h**

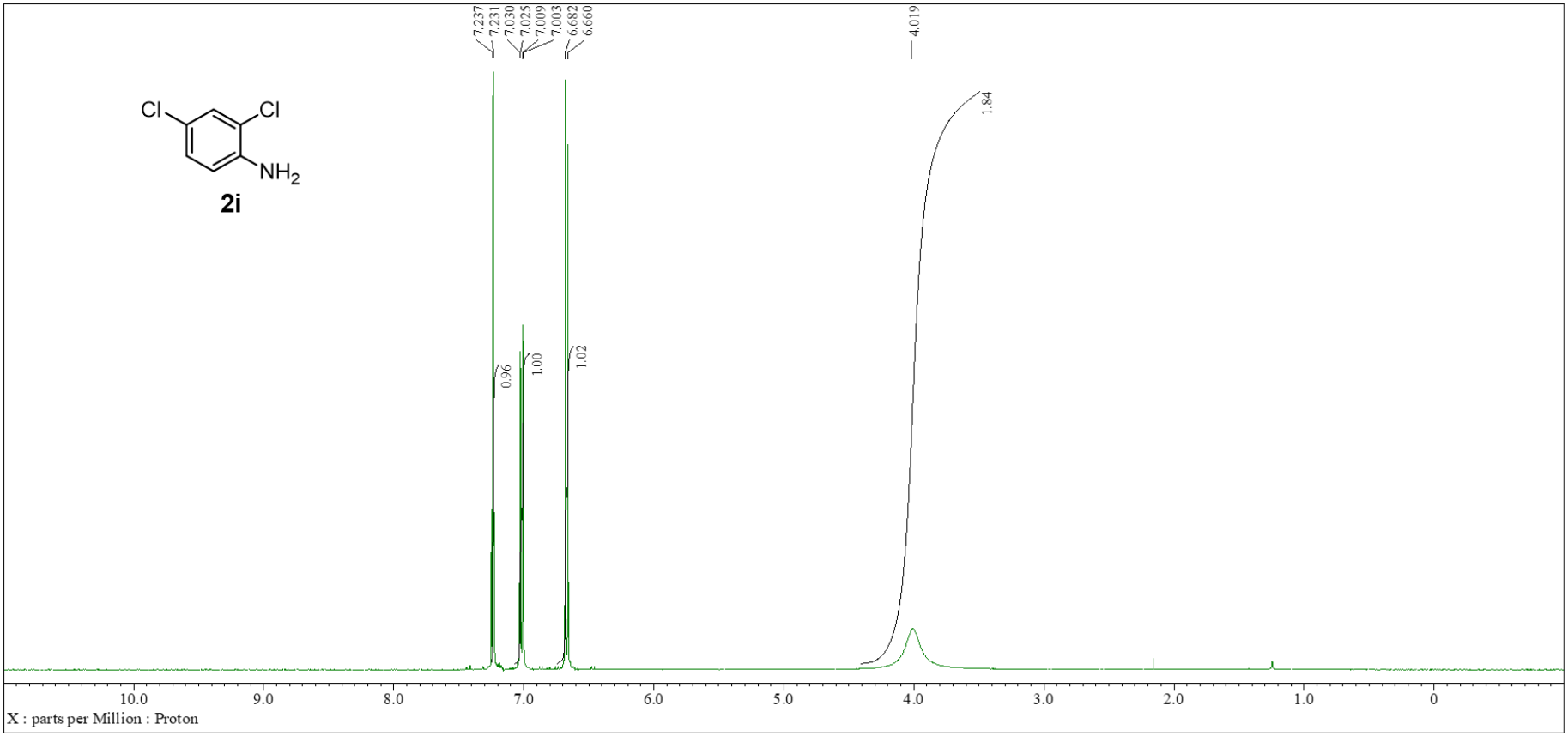
7.237
7.231
7.030
7.025
7.009
7.003
6.682
6.660
4.019
1.84
0.96
1.00
1.02
Cl
Cl
NH2
2i
10.0
9.0
8.0
7.0
6.0
5.0
4.0
3.0
2.0
1.0
0
X : parts per Million : Proton

^{1}H NMR of **2i**

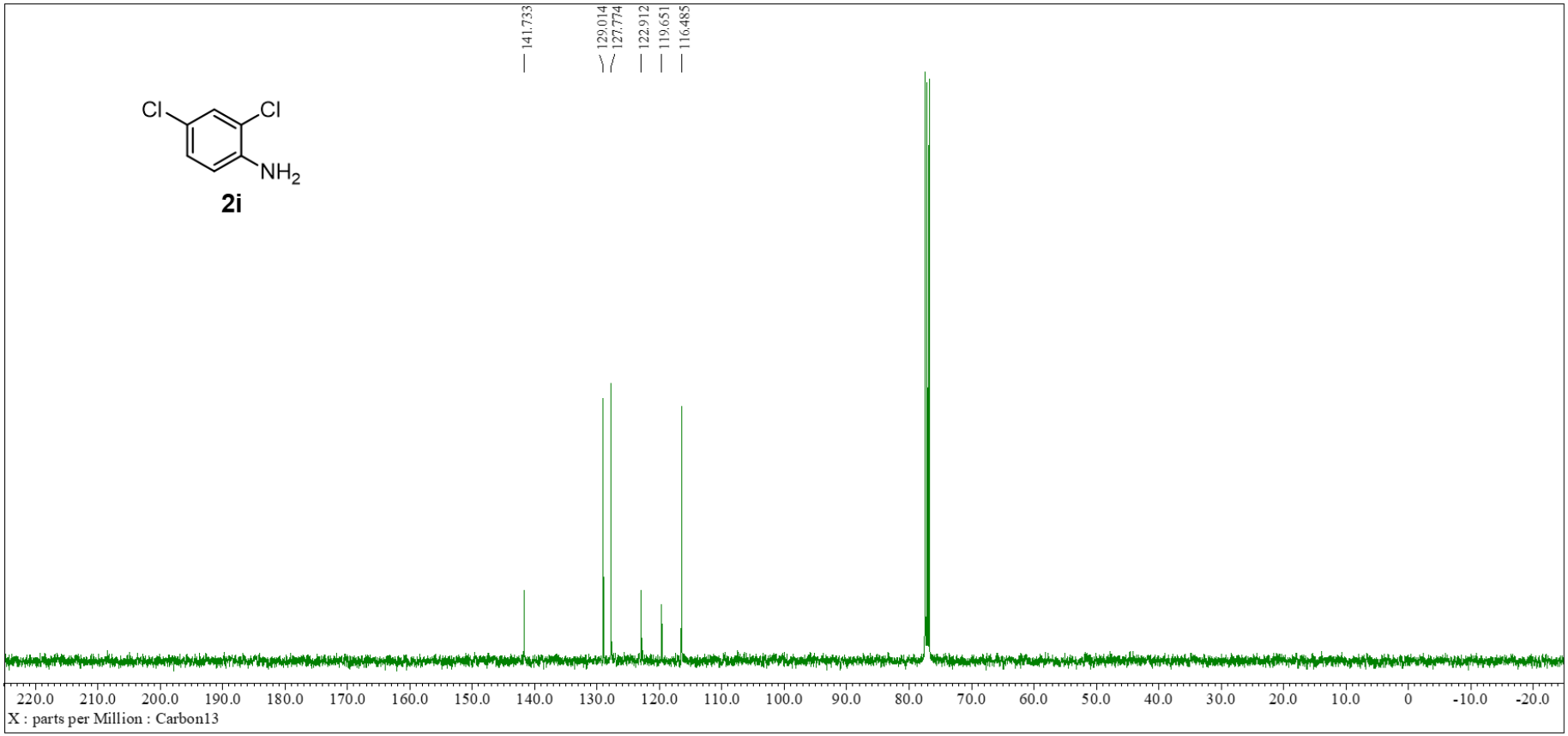
141.733
129.014
127.774
122.912
119.651
116.485
Cl
Cl
NH2
2i
220.0 210.0 200.0 190.0 180.0 170.0 160.0 150.0 140.0 130.0 120.0 110.0 100.0 90.0 80.0 70.0 60.0 50.0 40.0 30.0 20.0 10.0 0 -10.0 -20.0
X : parts per Million : Carbon13

^{13}C NMR of **2i**

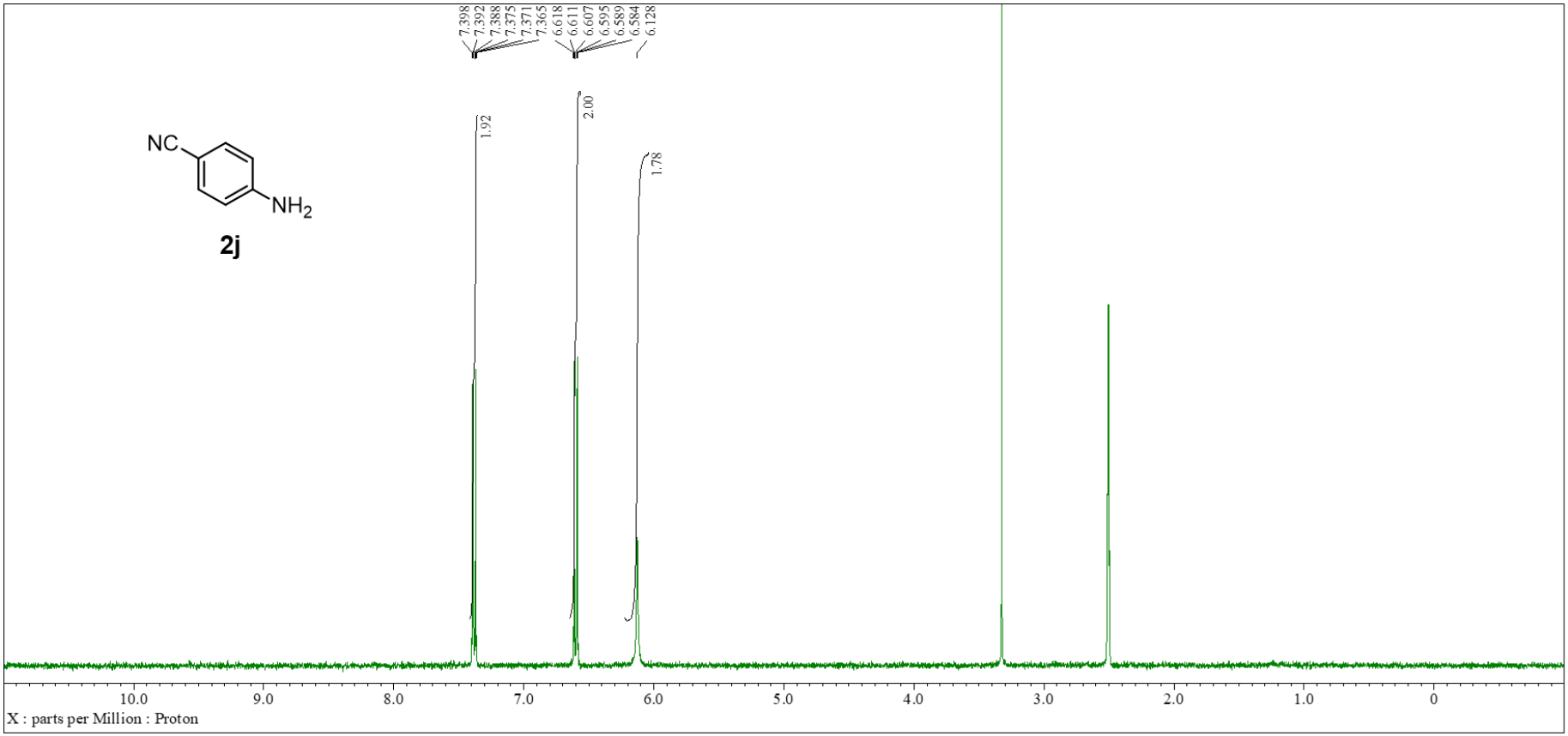
7.398
7.392
7.388
7.375
7.371
7.365
6.618
6.611
6.607
6.595
6.589
6.584
6.128
1.92
2.00
1.78
NC
NH2
2j
10.0
9.0
8.0
7.0
6.0
5.0
4.0
3.0
2.0
1.0
0
X : parts per Million : Proton

^{1}H NMR of **2j**

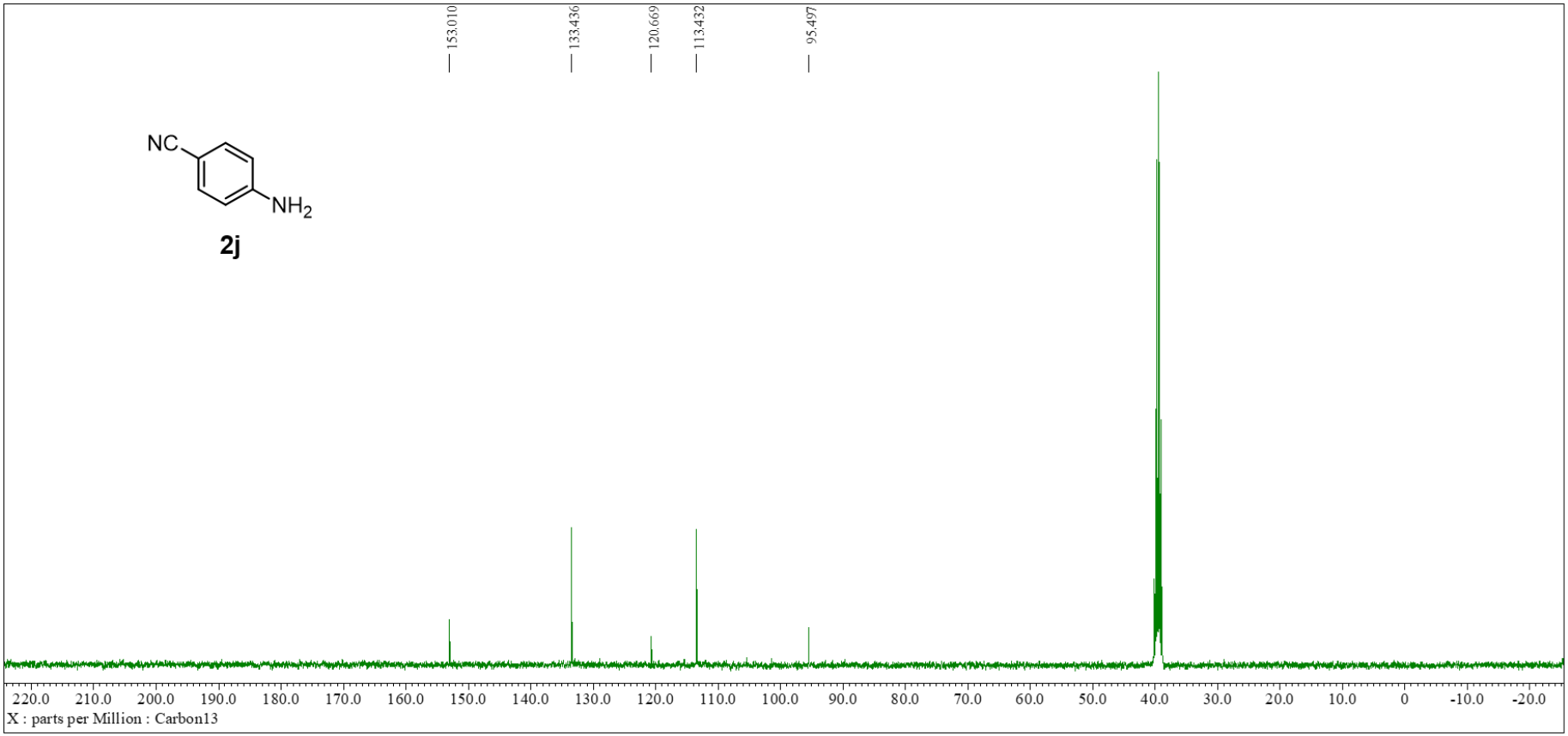
153.010
133.436
120.669
113.432
95.497
NC
NH2
2j
220.0 210.0 200.0 190.0 180.0 170.0 160.0 150.0 140.0 130.0 120.0 110.0 100.0 90.0 80.0 70.0 60.0 50.0 40.0 30.0 20.0 10.0 0 -10.0 -20.0
X : parts per Million : Carbon13

^{13}C NMR of **2j**

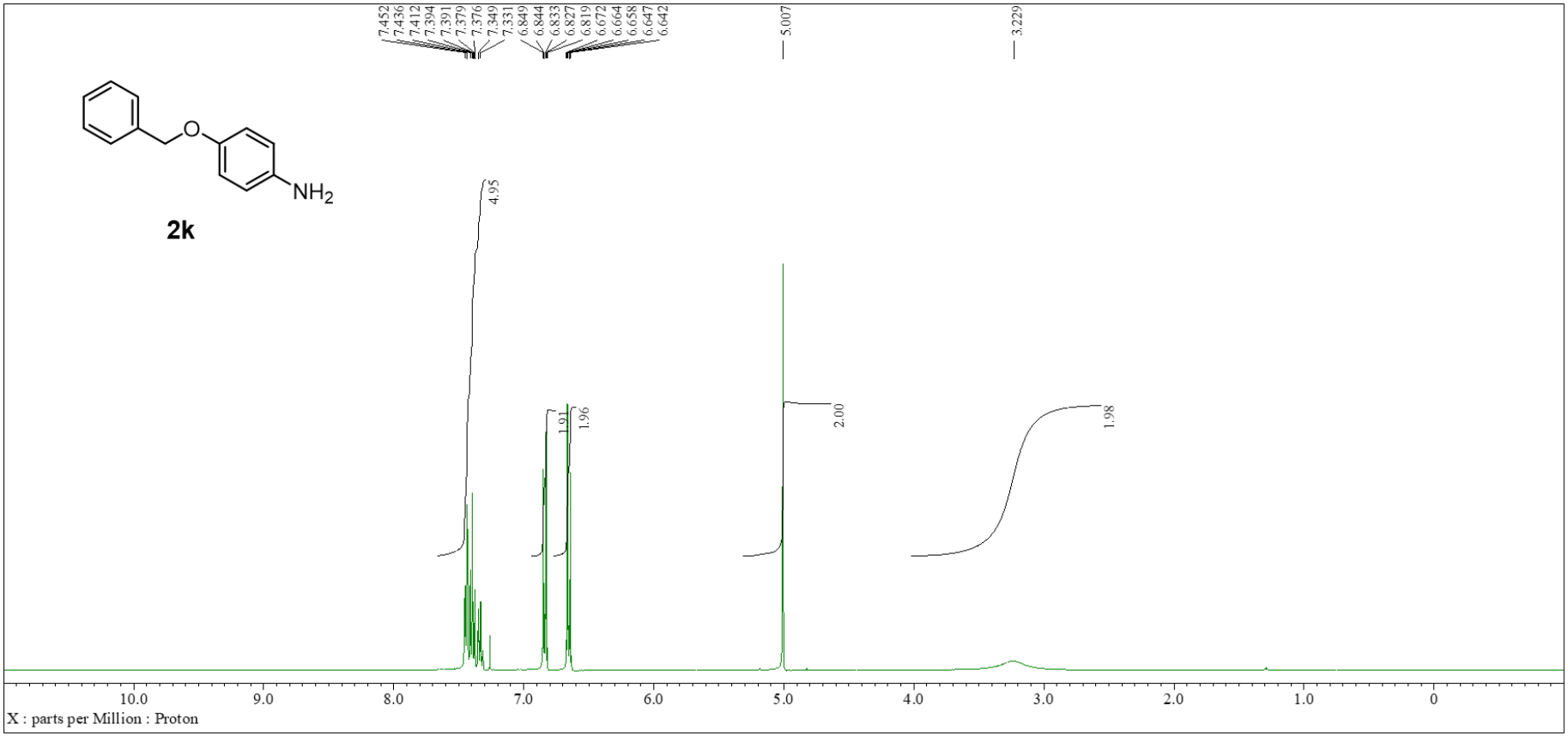
7.452
7.436
7.412
7.394
7.391
7.379
7.376
7.349
7.331
6.849
6.844
6.833
6.827
6.819
6.672
6.664
6.658
6.647
6.642
5.007
3.229
O
NH2
2k
4.95
1.91
1.96
2.00
1.98
10.0
9.0
8.0
7.0
6.0
5.0
4.0
3.0
2.0
1.0
0
X : parts per Million : Proton

^{1}H NMR of **2k**

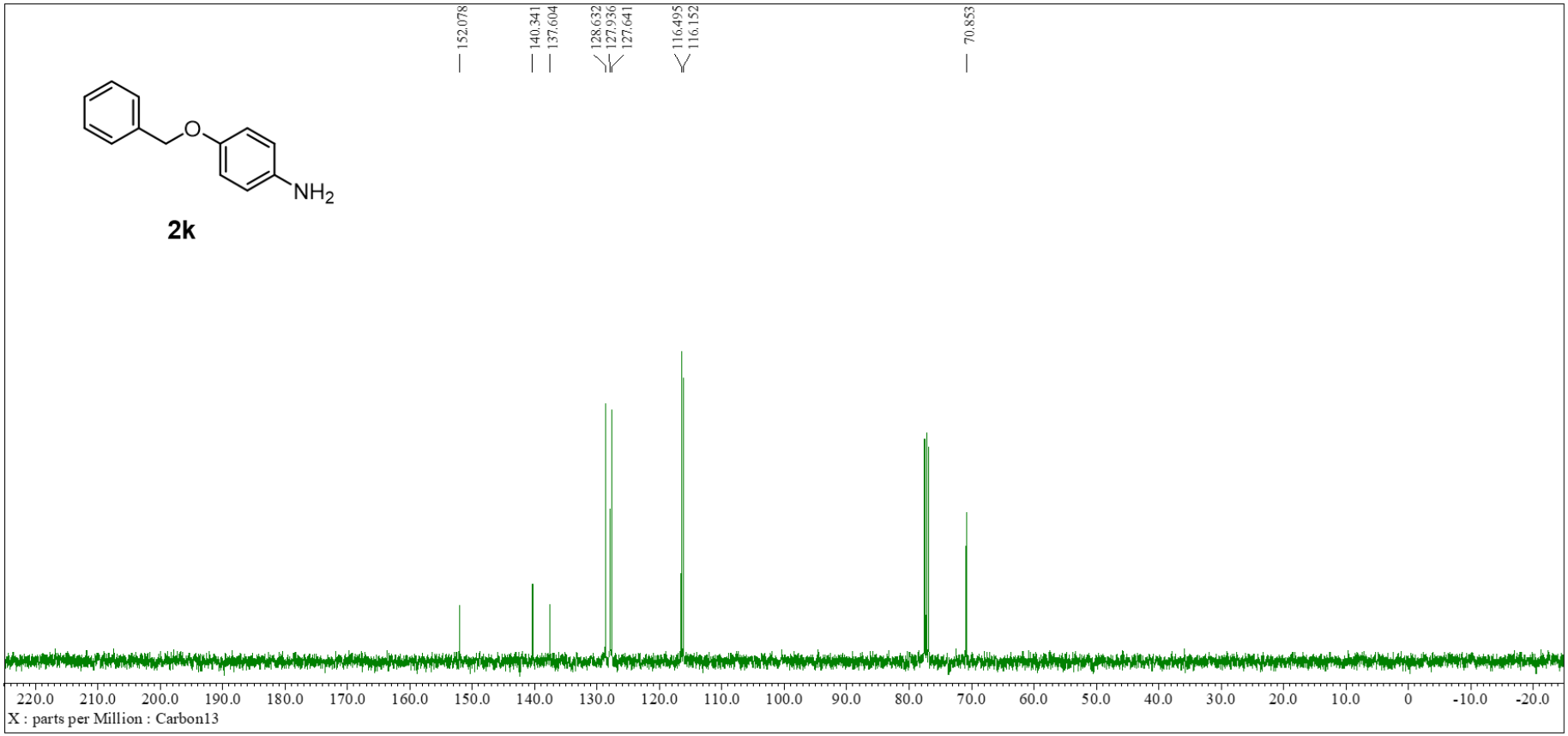
152.078
140.341
137.604
128.632
127.936
127.641
116.495
116.152
70.853
O
NH2
2k
220.0 210.0 200.0 190.0 180.0 170.0 160.0 150.0 140.0 130.0 120.0 110.0 100.0 90.0 80.0 70.0 60.0 50.0 40.0 30.0 20.0 10.0 0 -10.0 -20.0
X : parts per Million : Carbon13

^{13}C NMR of **2k**

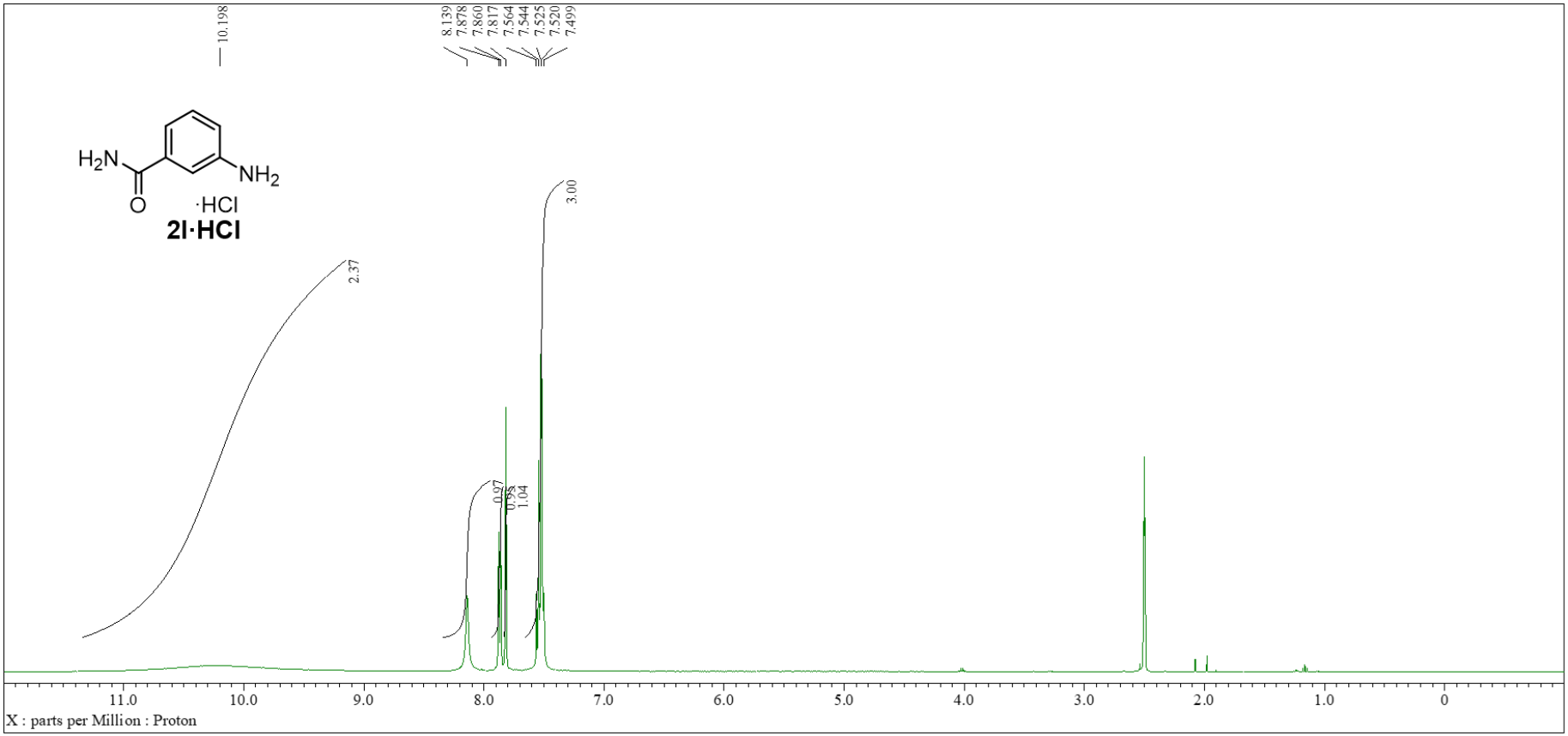

^{1}H NMR of **2l·HCl**

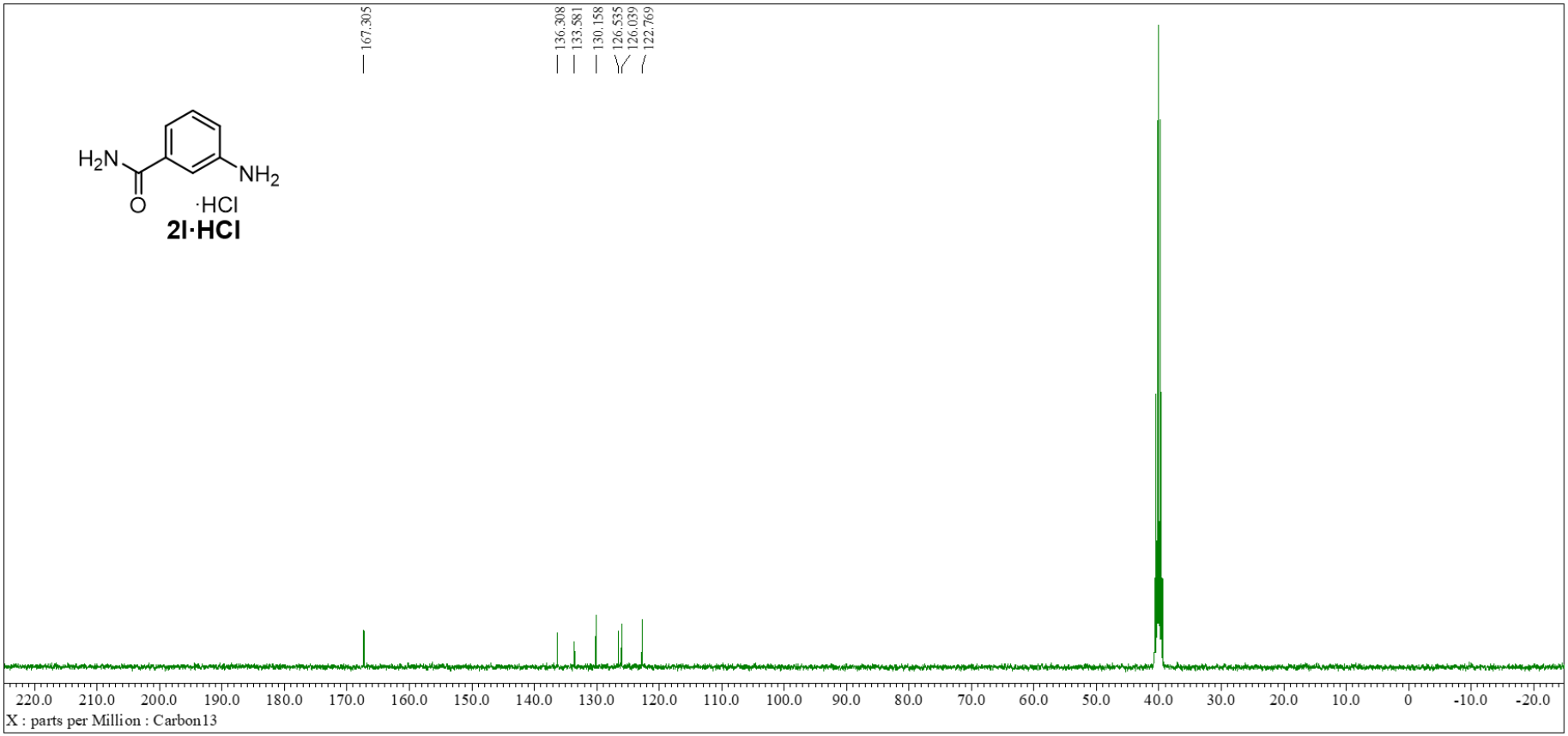

^{13}C NMR of **2l·HCl**

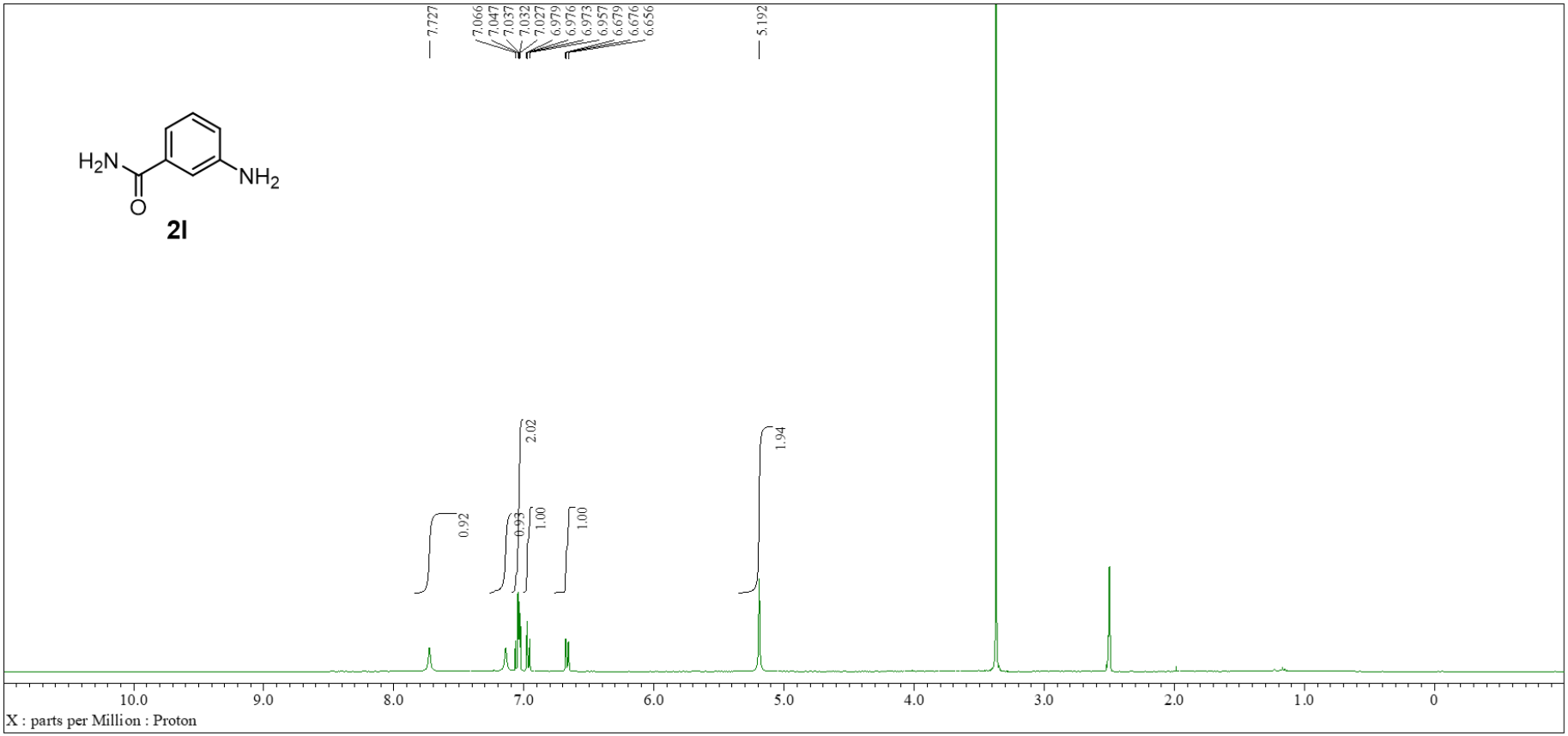
7.727
7.066
7.047
7.037
7.032
7.027
6.979
6.976
6.973
6.957
6.679
6.676
6.656
5.192
H2N
NH2
O
21
0.92
0.93
2.02
1.00
1.00
1.94
10.0
9.0
8.0
7.0
6.0
5.0
4.0
3.0
2.0
1.0
0
X : parts per Million : Proton

^{1}H NMR of **21**

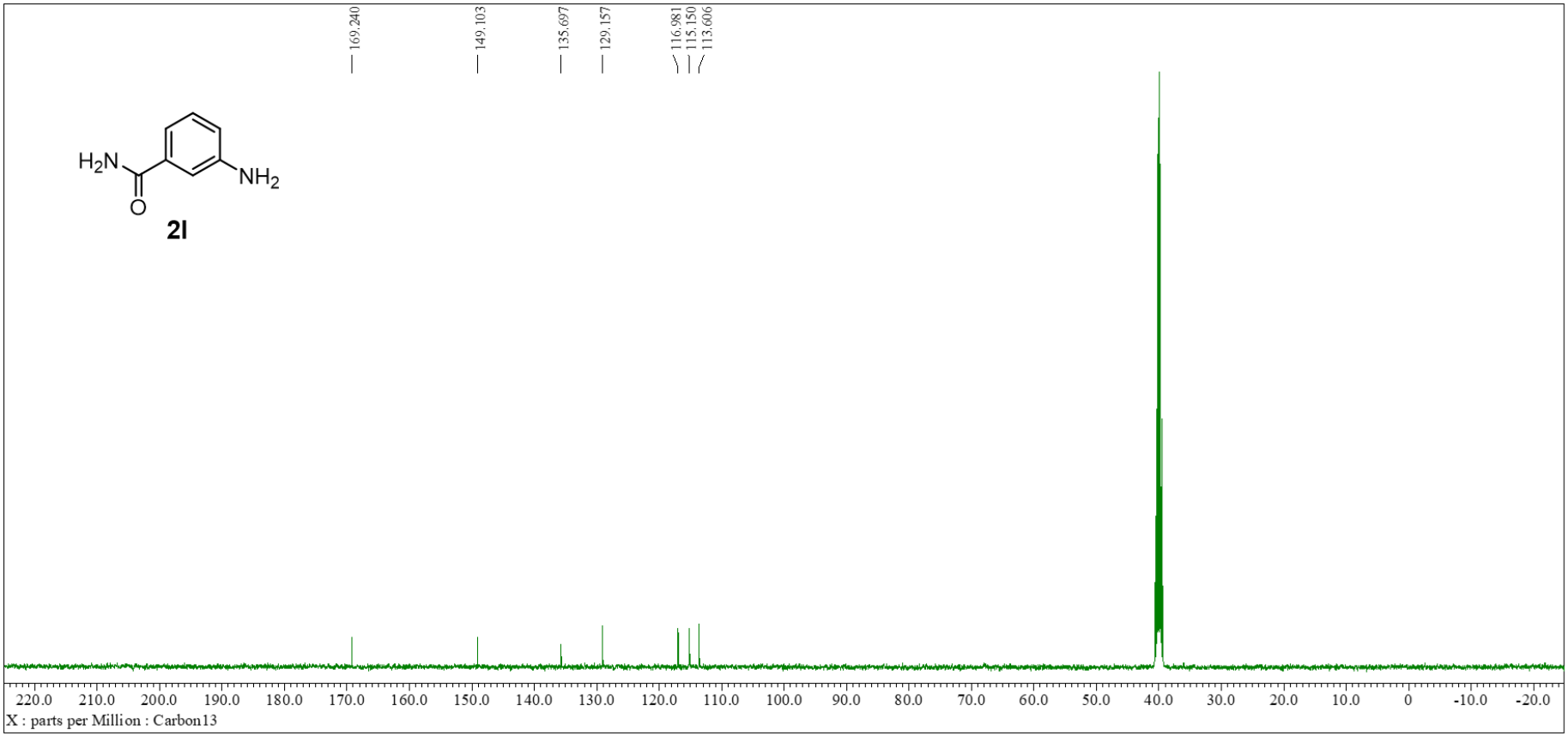
169.240
149.103
135.697
129.157
116.981
115.150
113.606
H2N
NH2
O
2l
220.0 210.0 200.0 190.0 180.0 170.0 160.0 150.0 140.0 130.0 120.0 110.0 100.0 90.0 80.0 70.0 60.0 50.0 40.0 30.0 20.0 10.0 0 -10.0 -20.0
X : parts per Million : Carbon13

^{13}C NMR of **2l**

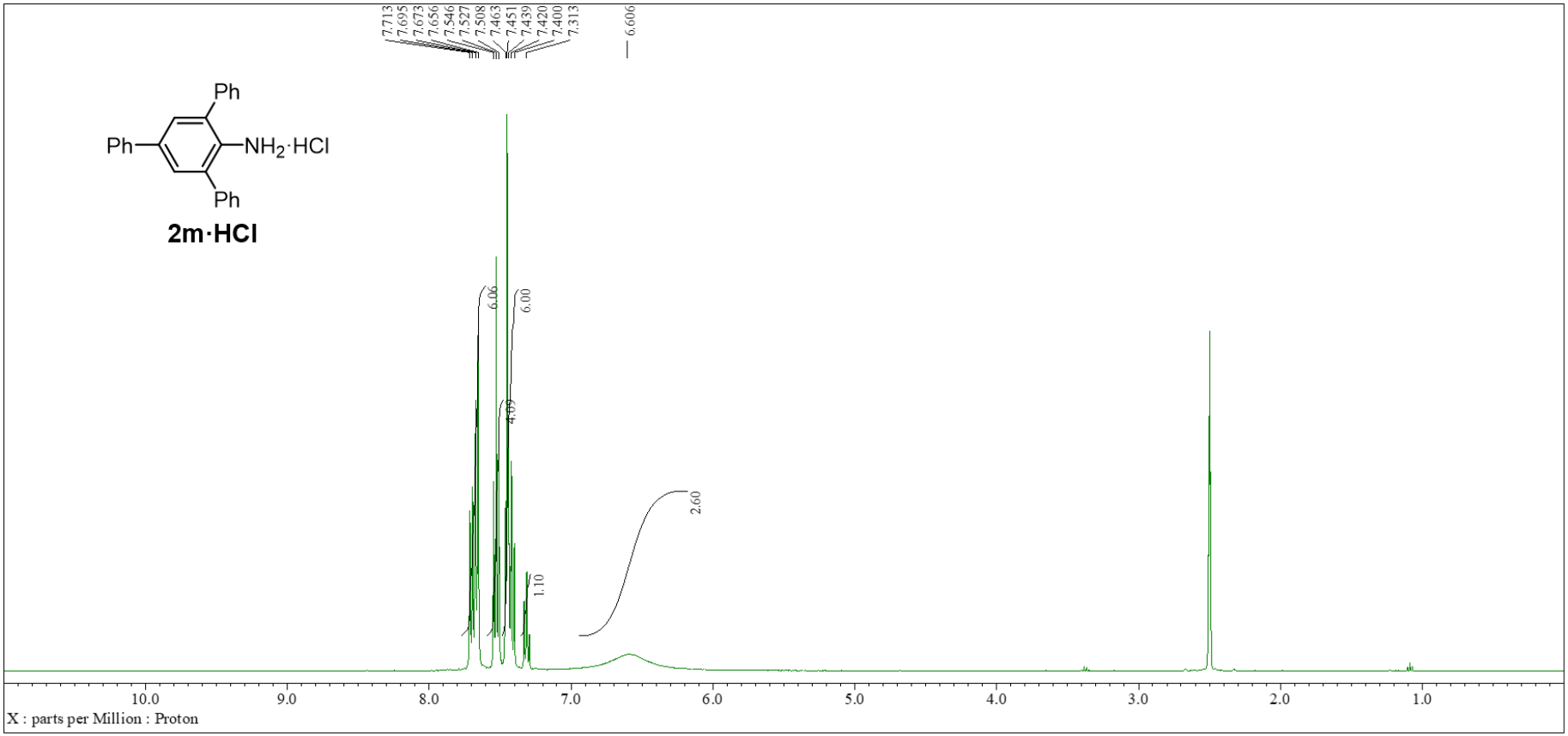

^{1}H NMR of **2m·HCl**

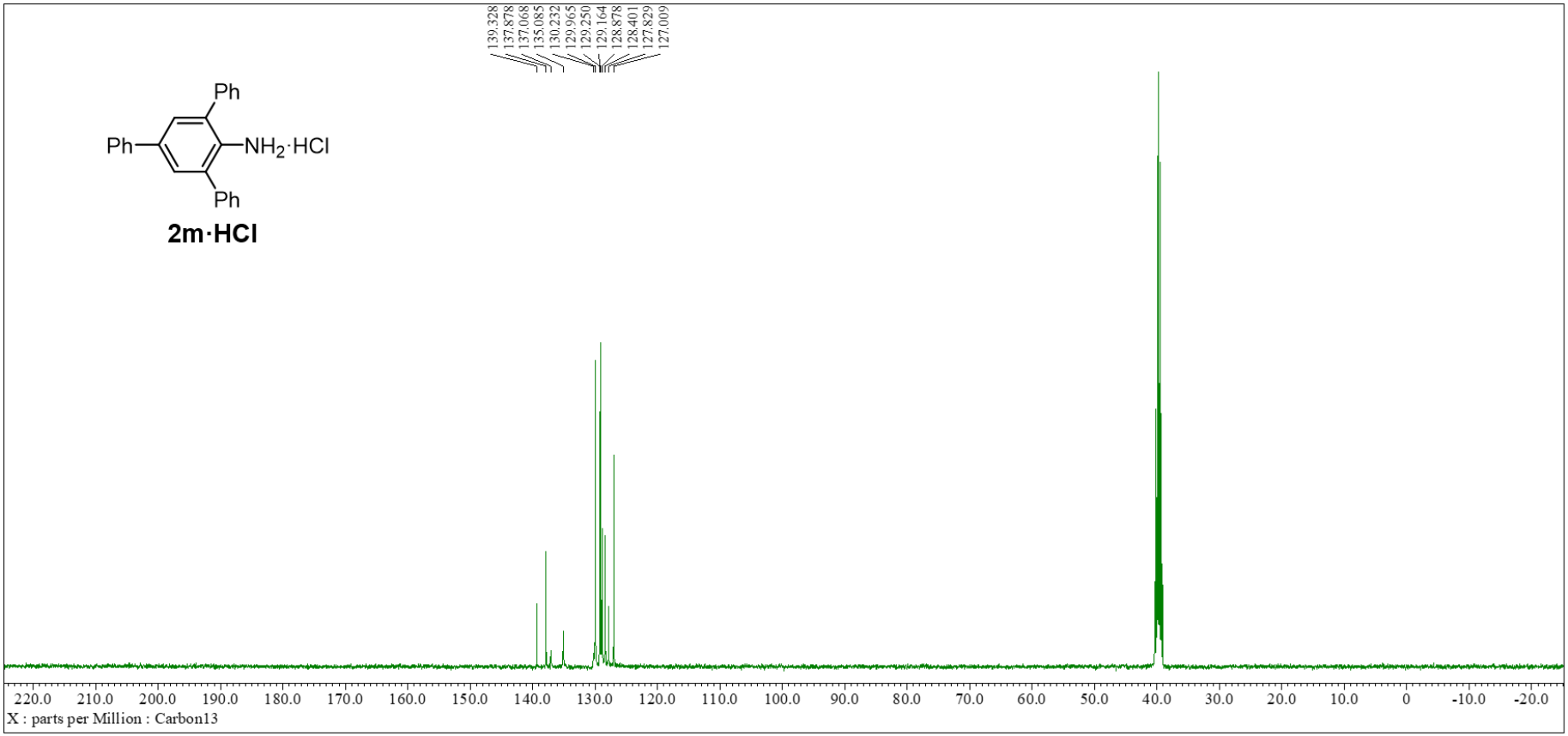

^{13}C NMR of **2m·HCl**

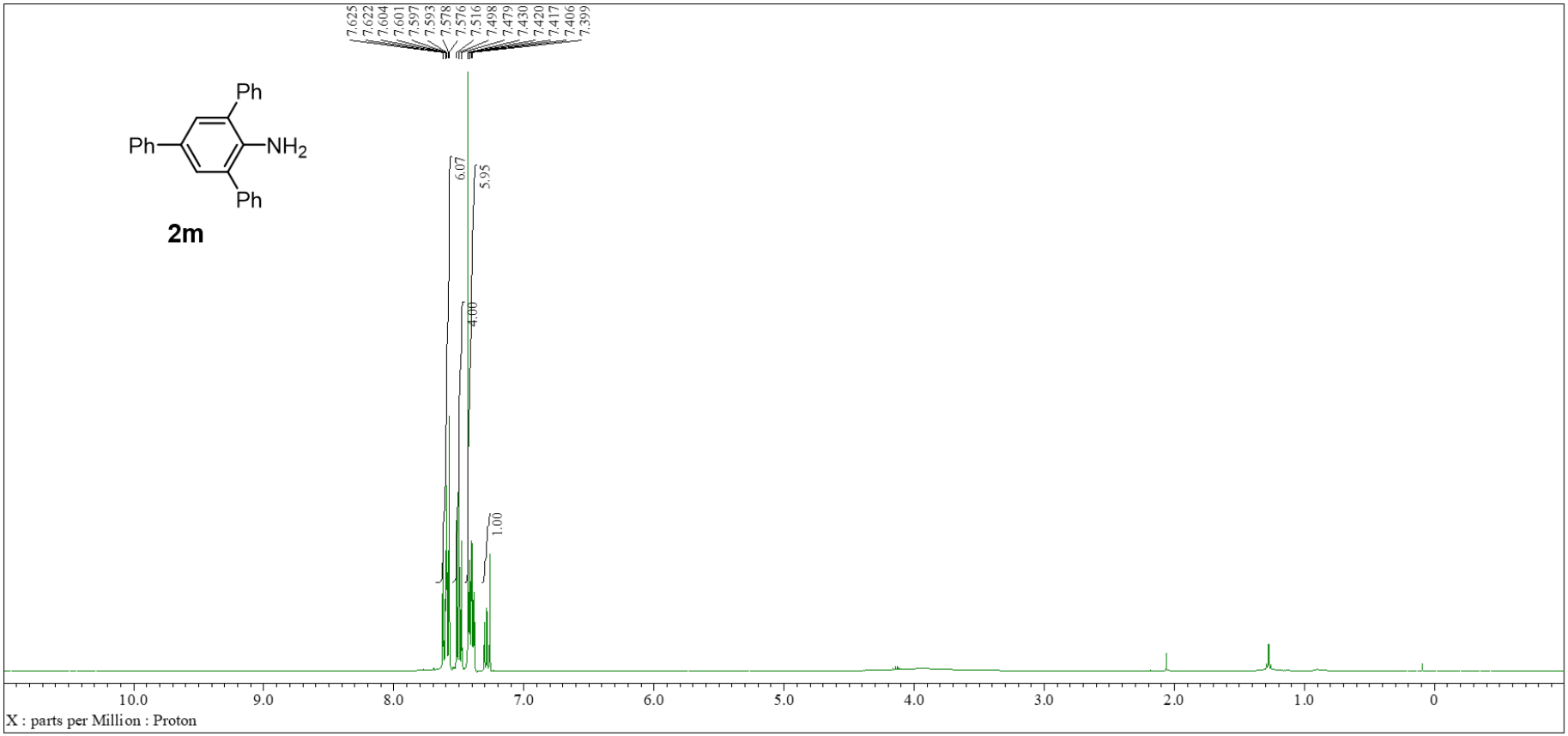
7.625
7.622
7.604
7.601
7.597
7.593
7.578
7.576
7.516
7.498
7.479
7.430
7.420
7.417
7.406
7.399
Ph
Ph
NH2
Ph
2m
6.07
5.95
4.00
1.00
10.0
9.0
8.0
7.0
6.0
5.0
4.0
3.0
2.0
1.0
0
X : parts per Million : Proton

^{1}H NMR of **2m**

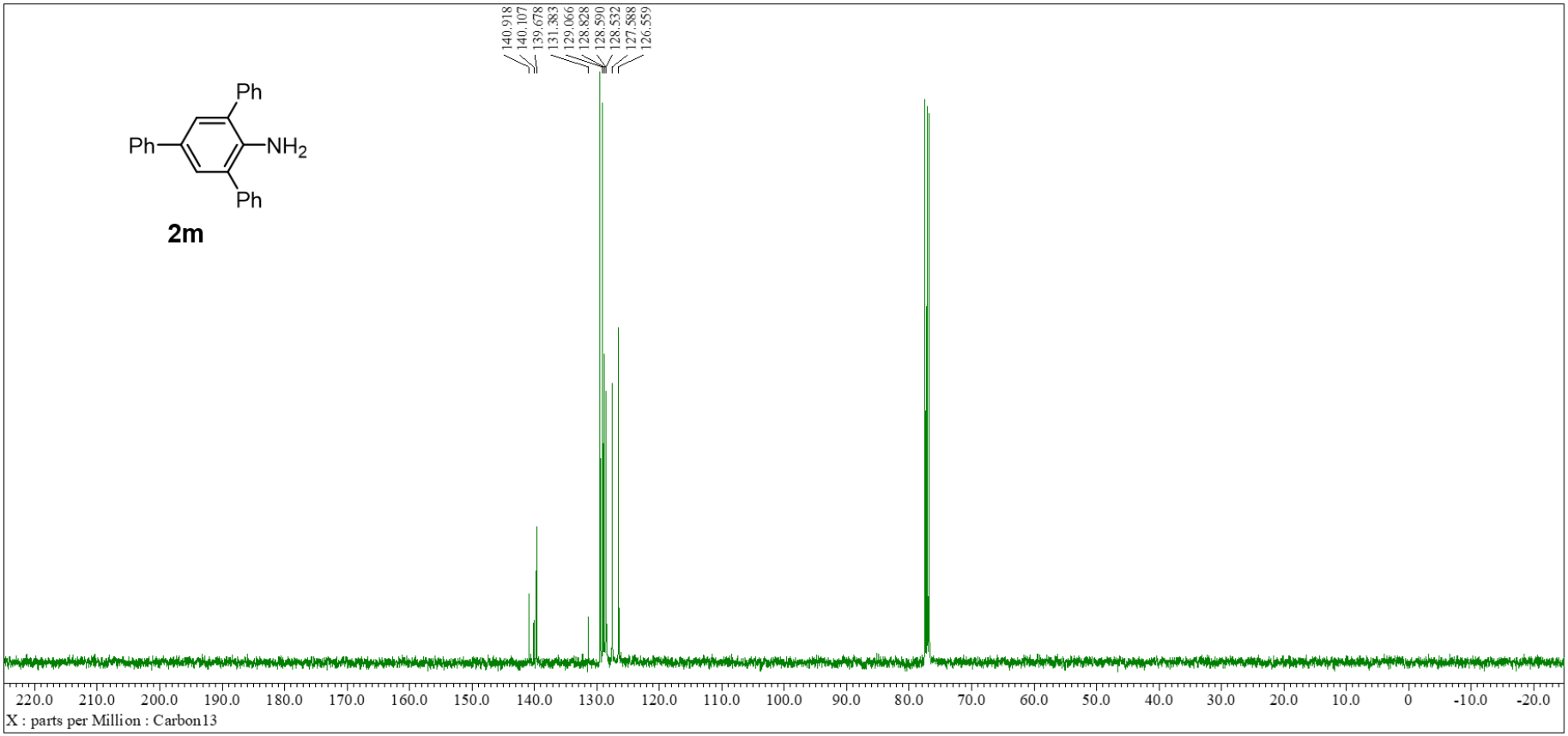
140.918
140.107
139.678
131.383
129.066
128.828
128.590
128.532
127.588
126.559
Ph
Ph
NH2
Ph
2m
220.0 210.0 200.0 190.0 180.0 170.0 160.0 150.0 140.0 130.0 120.0 110.0 100.0 90.0 80.0 70.0 60.0 50.0 40.0 30.0 20.0 10.0 0 -10.0 -20.0
X : parts per Million : Carbon13

^{13}C NMR of **2m**

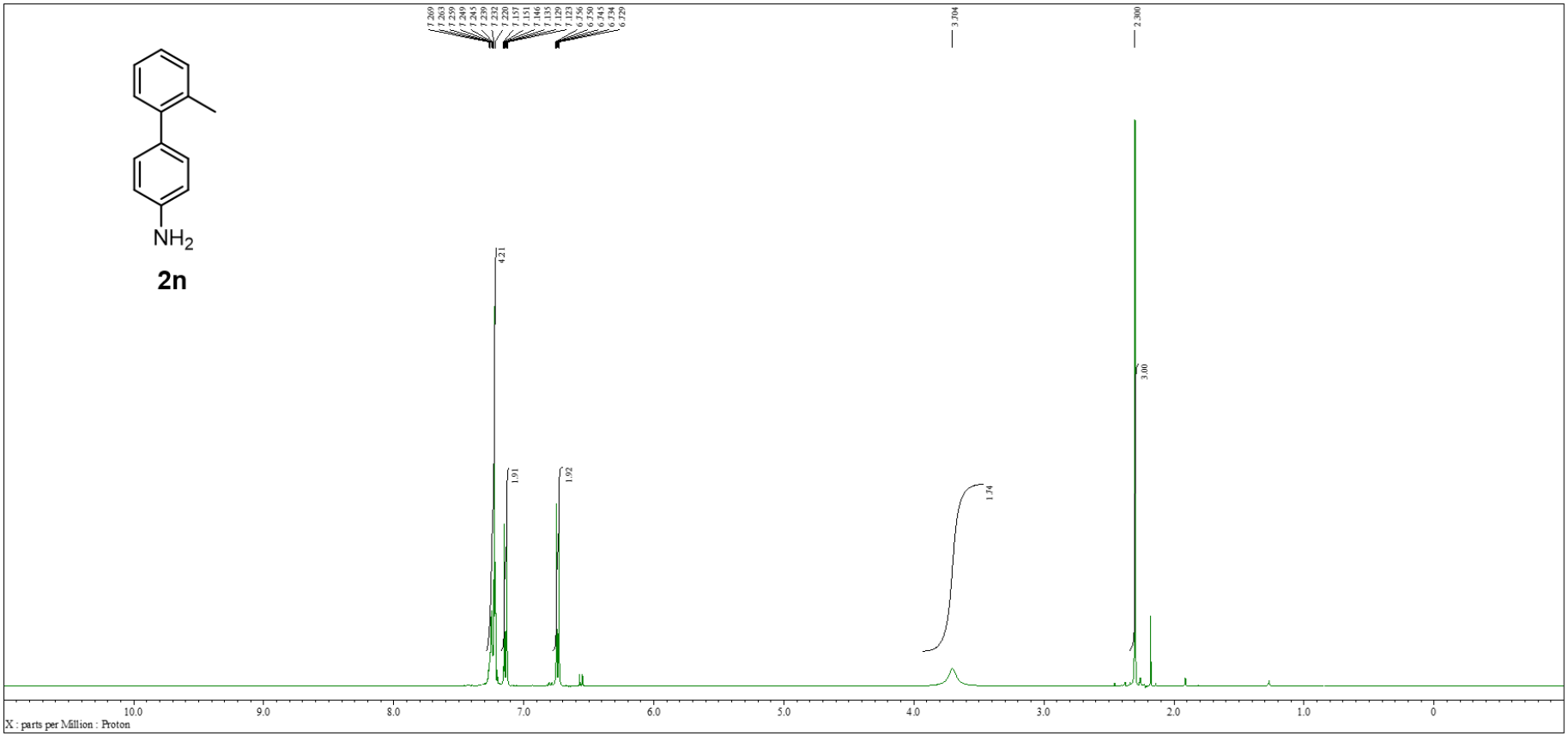
NH2
2n
7.269
7.263
7.259
7.249
7.245
7.239
7.232
7.220
7.157
7.151
7.146
7.135
7.129
7.123
6.756
6.750
6.745
6.734
6.729
3.704
2.300
4.21
1.91
1.92
1.34
3.00
10.0
9.0
8.0
7.0
6.0
5.0
4.0
3.0
2.0
1.0
0
X : parts per Million : Proton

^{1}H NMR of **2n**

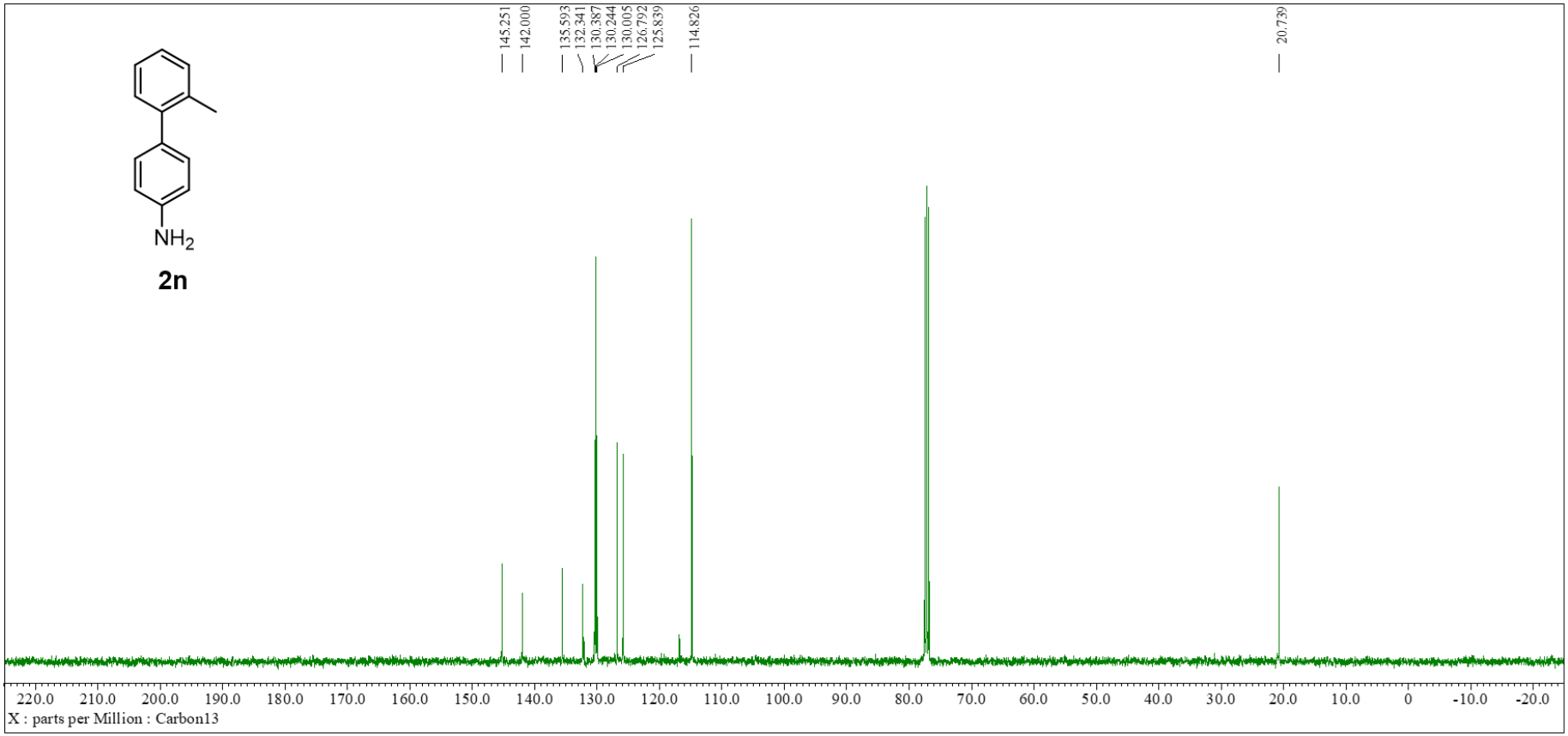
145.251
142.000
135.593
132.341
130.387
130.244
130.005
126.792
125.839
114.826
20.739
NH2
2n
220.0 210.0 200.0 190.0 180.0 170.0 160.0 150.0 140.0 130.0 120.0 110.0 100.0 90.0 80.0 70.0 60.0 50.0 40.0 30.0 20.0 10.0 0 -10.0 -20.0
X : parts per Million : Carbon13

^{13}C NMR of **2n**

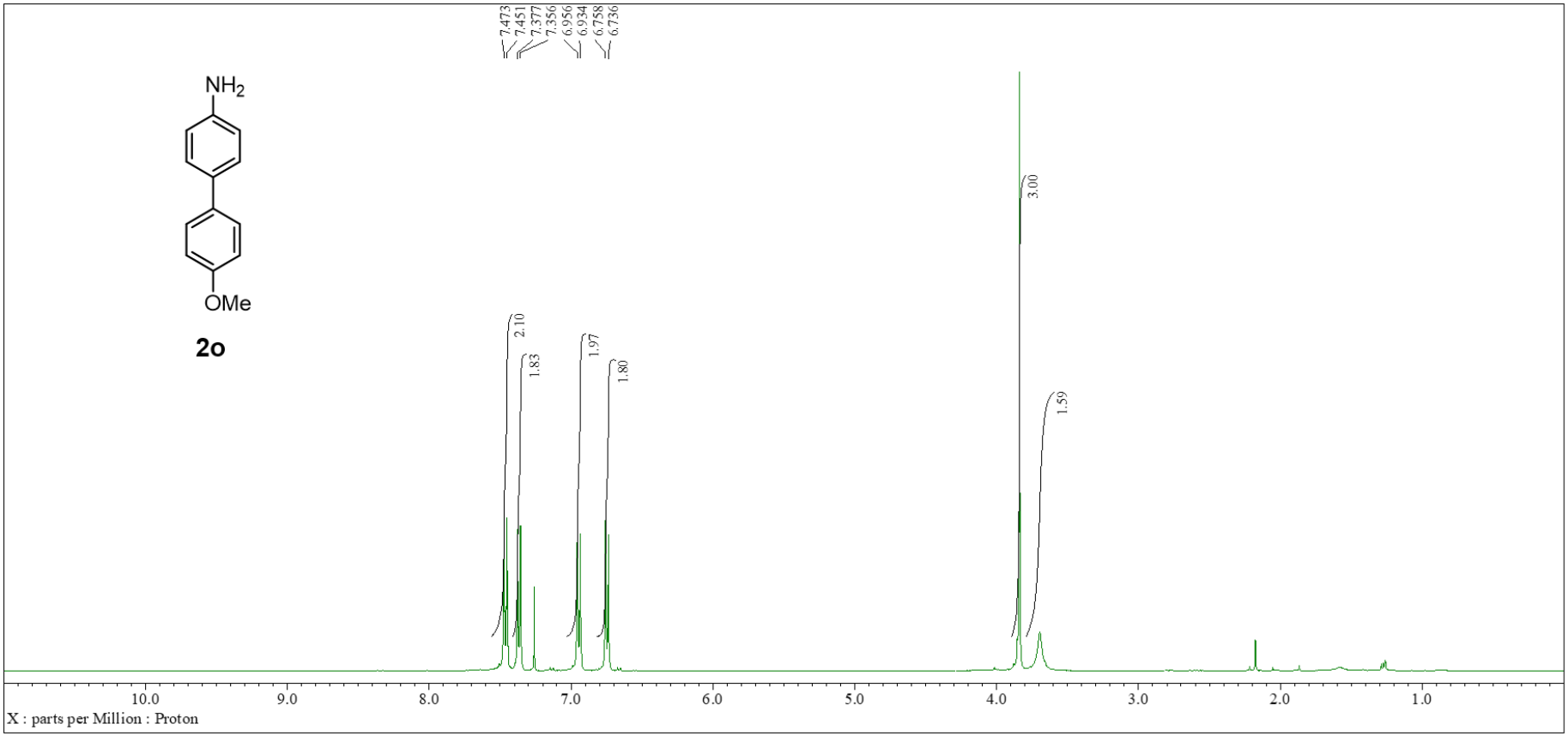
7.473
7.451
7.377
7.356
6.956
6.934
6.758
6.736
NH2
OMe
2o
2.10
1.83
1.97
1.80
3.00
1.59
10.0
9.0
8.0
7.0
6.0
5.0
4.0
3.0
2.0
1.0
X : parts per Million : Proton

^{1}H NMR of **2o**

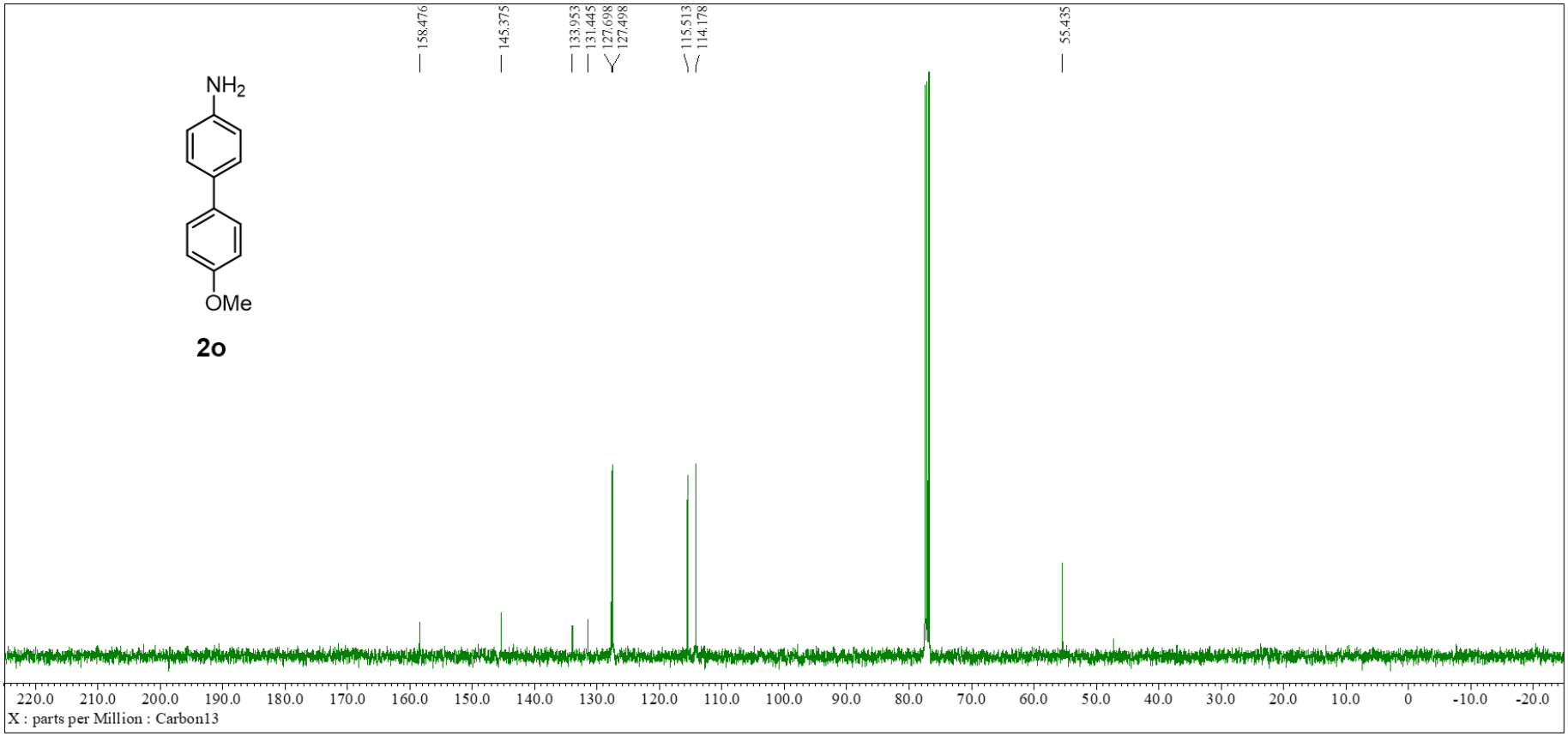
158.476
145.375
133.953
131.445
127.698
127.498
115.513
114.178
55.435
NH2
OMe
2o
220.0 210.0 200.0 190.0 180.0 170.0 160.0 150.0 140.0 130.0 120.0 110.0 100.0 90.0 80.0 70.0 60.0 50.0 40.0 30.0 20.0 10.0 0 -10.0 -20.0
X : parts per Million : Carbon13

^{13}C NMR of **2o**